Optimization of the High-Intensity Muon Beamlines for MEG II, Mu3e and HIMB

Giovanni Dal Maso

PSI - ETH Zürich

Intense
H2020 MSCA ITN
G.A. 858199

Bachelor and Master degrees

- Born in Cuneo and grown up in Siena, Italy
- Bachelor in Physics at University of Pisa, 2015-2018
- Master in Fundamental Interactions at University of Pisa, 2018-2020. Thesis title: "Beam diagnostic and calibration tools for the MEGII experiment".
- Started Ph.D. at PSI - ETH Zürich on March 2021, finished on the 15th of March 2024.

giovanni.dal-maso@psi.ch

CMBL commissioning

Charged Lepton Flavor Violation

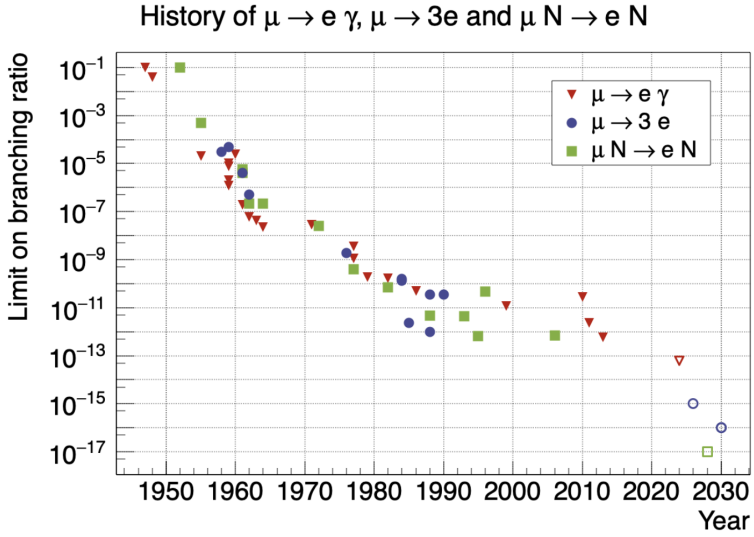

Charged Lepton Flavor Violation

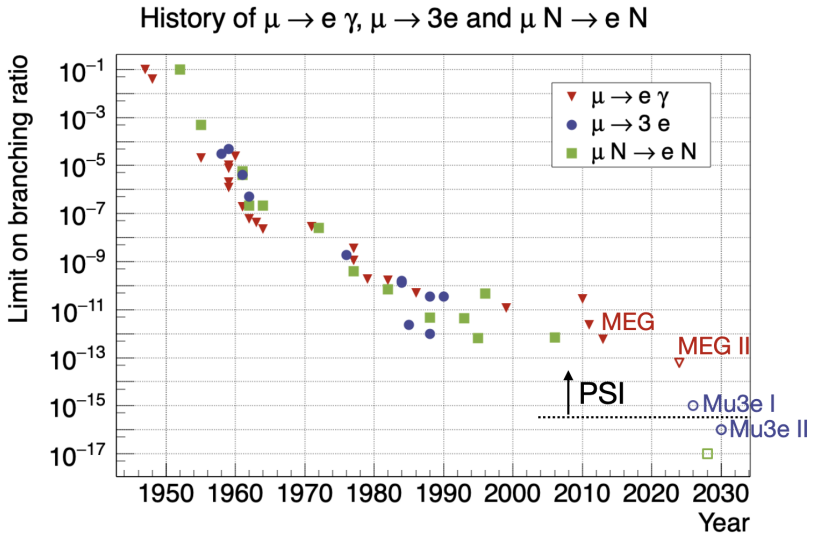

The High Intensity Proton Accelerator (HIPA) facility

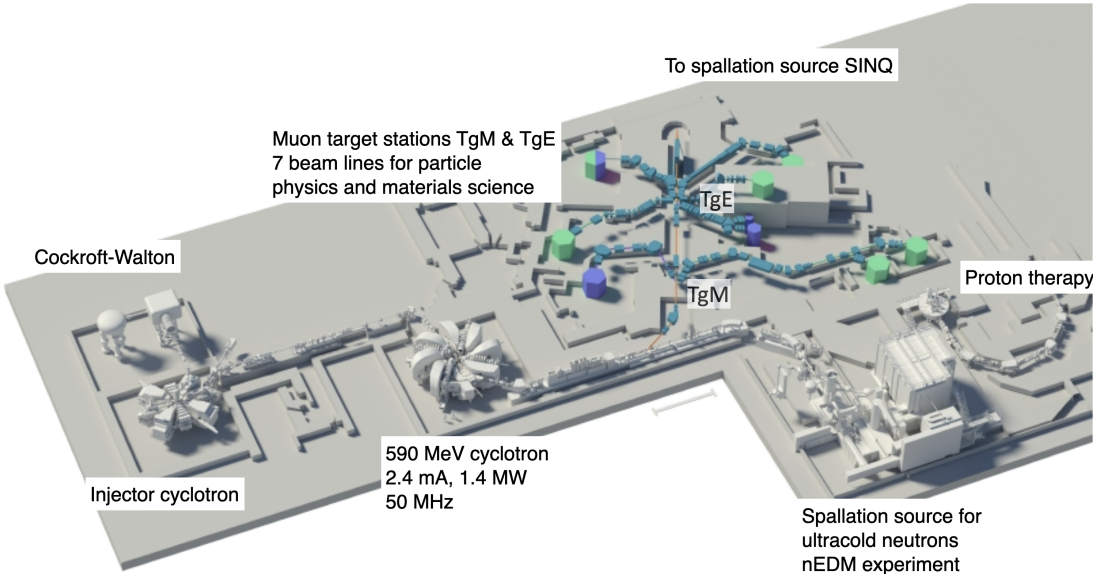

The High Intensity Proton Accelerator (HIPA) facility

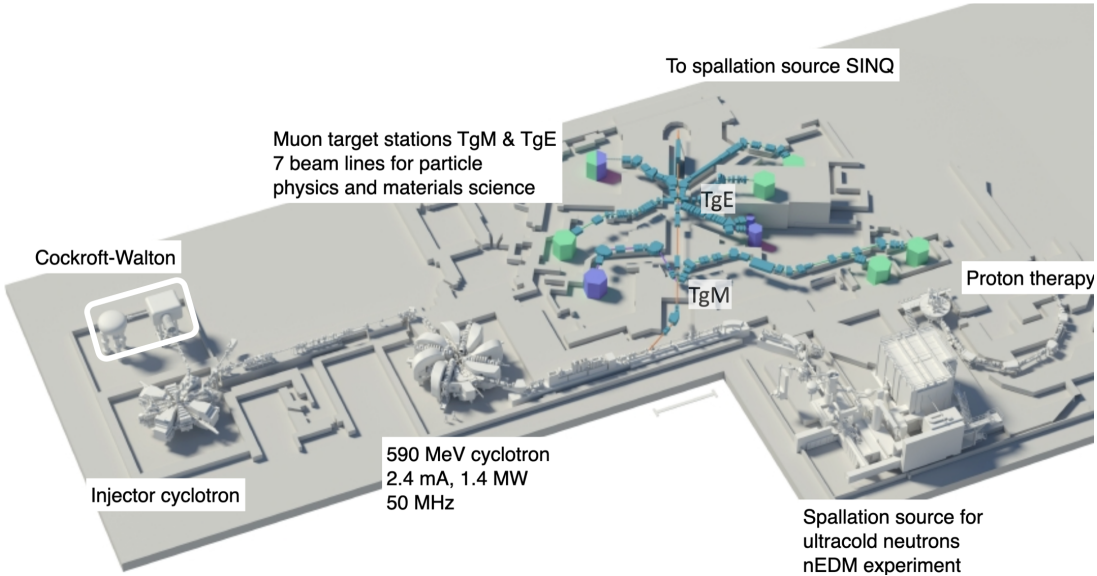

The High Intensity Proton Accelerator (HIPA) facility

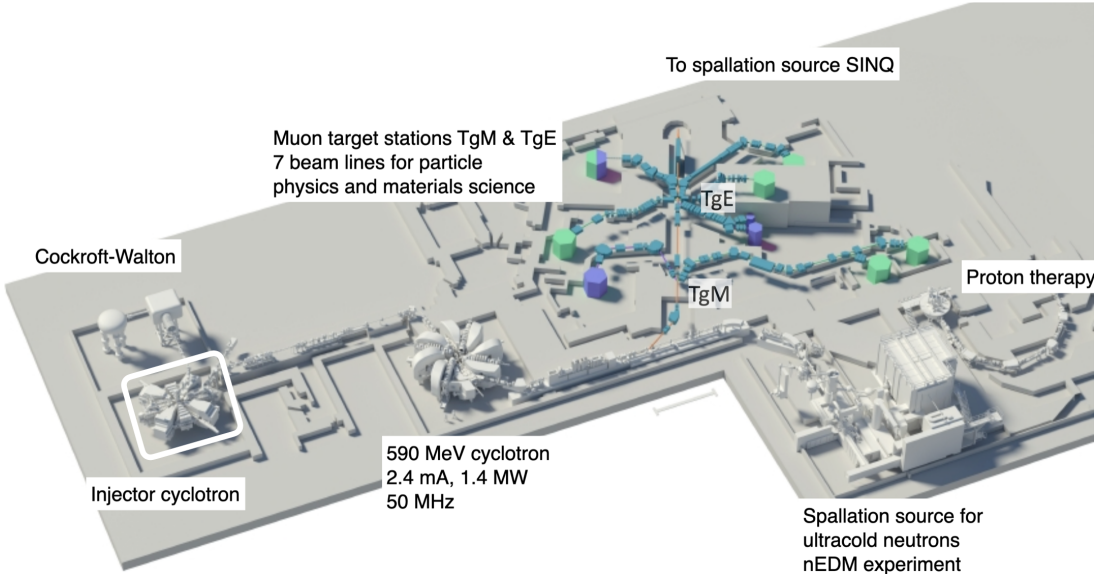

The High Intensity Proton Accelerator (HIPA) facility

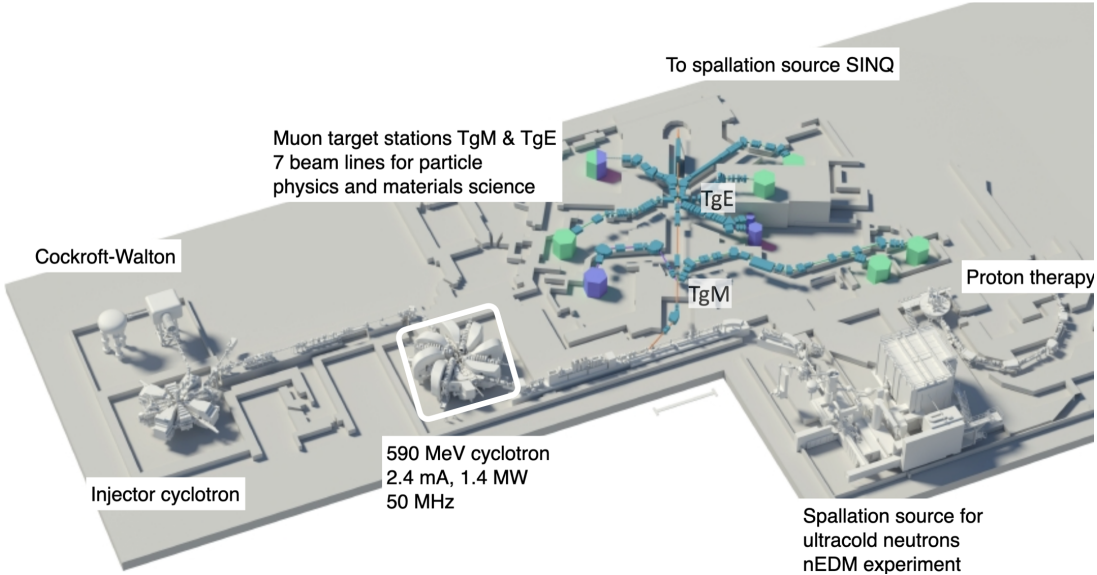

The High Intensity Proton Accelerator (HIPA) facility

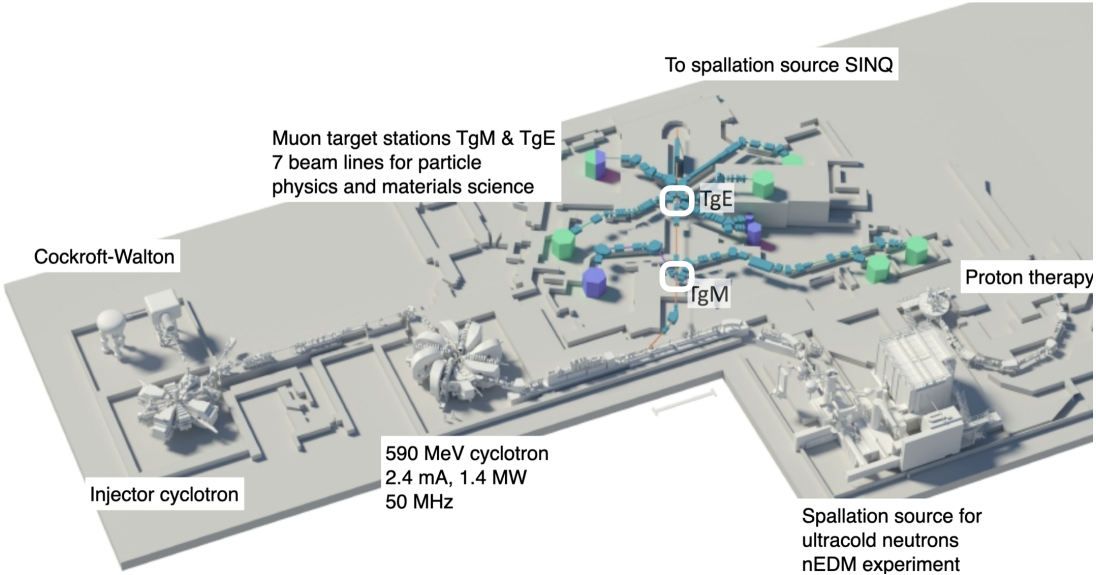

Muon production

The protons impinge on the targets, producing pions that decay in muons. Depending on where they are created, we classify:

- Surface and sub-surface muons (5-30 MeV/c): pion decay at rest.
- Cloud muons: pion decay in flight.

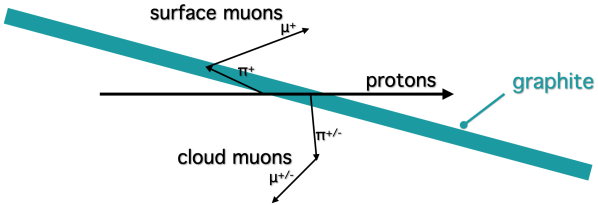

Due to the high intensity and low momentum, the most interesting muons for many experimental applications are surface muons as they can be stopped in low material budget targets.

Muon production

- **Surface and sub-surface muons (5-30 MeV/c): pion decay at rest.**

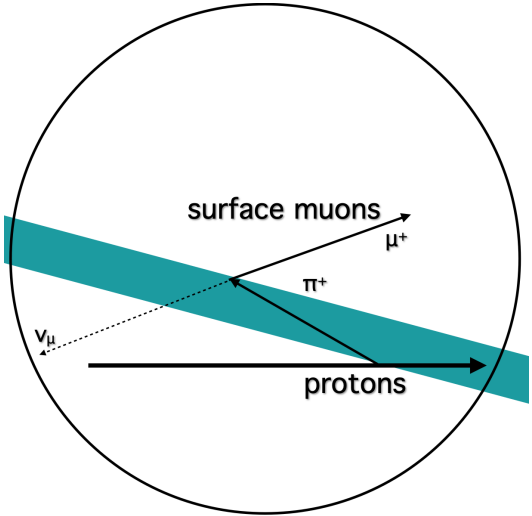

Muon production

- **Cloud muons: pion decay in flight.**

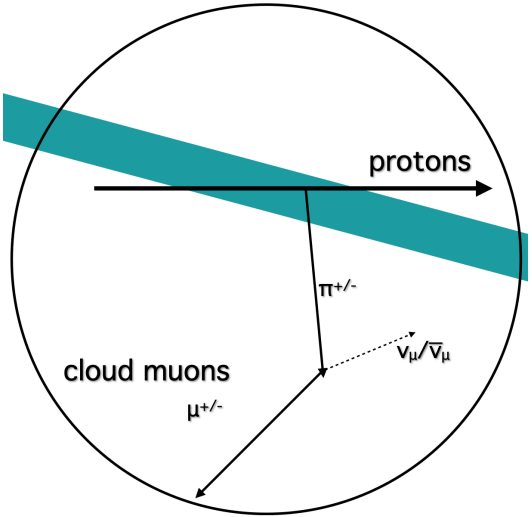

Muon production

The protons impinge on the targets, producing pions that decay in muons. Depending on where they are created, we classify:

- Surface and sub-surface muons (5-30 MeV/c): pion decay at rest.
- Cloud muons: pion decay in flight.

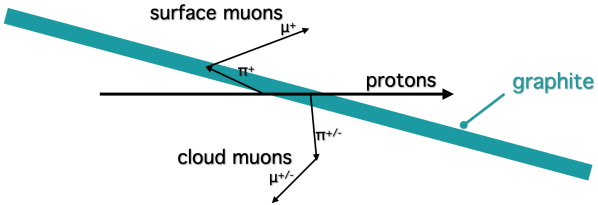

Due to the high intensity and low momentum, the most interesting muons for many experimental applications are surface muons as they can be stopped in low material budget targets.

The High Intensity Proton Accelerator (HIPA) facility

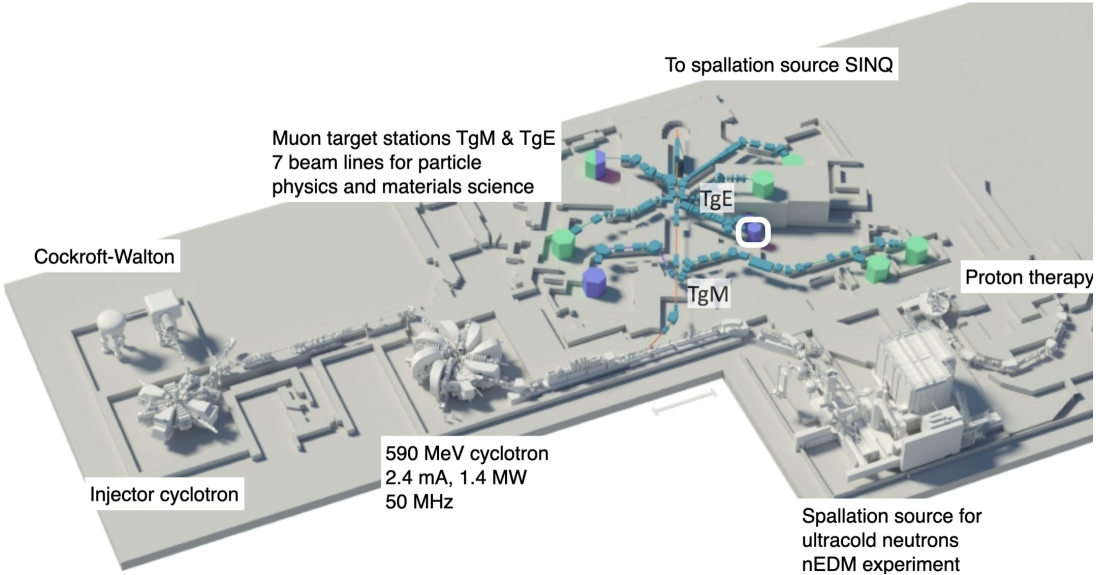

πE5

The πE5 beamline delivers the highest muon intensities up to 2×10^8 μ^+/s.The front part is shared between Mu3e and MEG II.

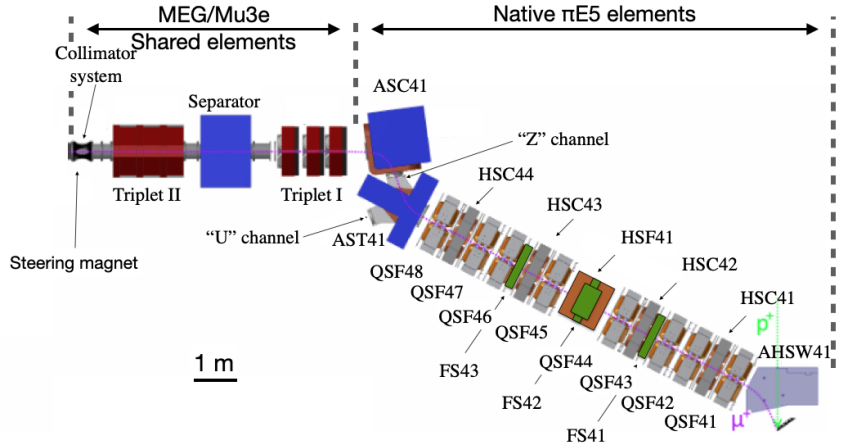

The Compact Muon Beam Line

The MEG II experiment is permanently installed in the DS part of the πE5 area
→ **need for a compact solution!**

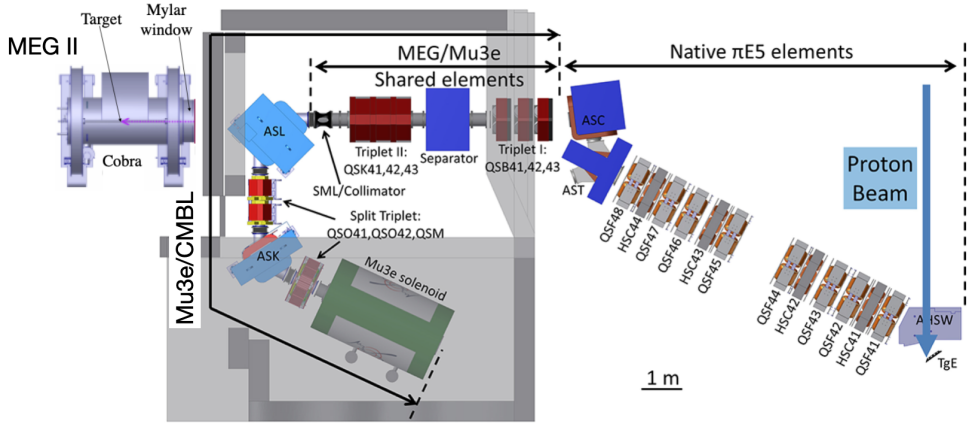

The Compact Muon Beam Line

The MEG II experiment is permanently installed in the DS part of the πE5 area
→ **need for a compact solution!**

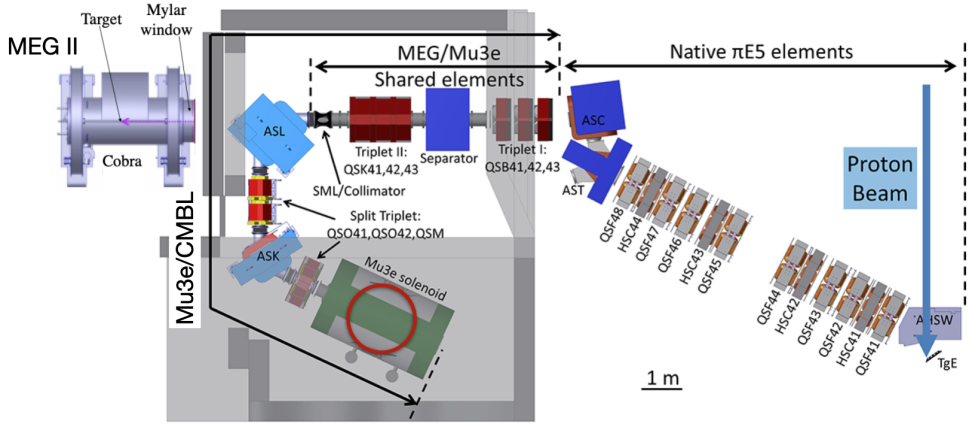

Beamline status and results

CMBL commissioning rates comparison	
	Rate [μ^+/s] @ 2.2 mA
Year	Mu3e center
2021	4.40 10^7
2022	6.89 10^7
2023	7.50 10^7*
TDR	6-7 10^7

Table: In 2023 (*), the measurement at Mu3e center was performed with the moderator in place.

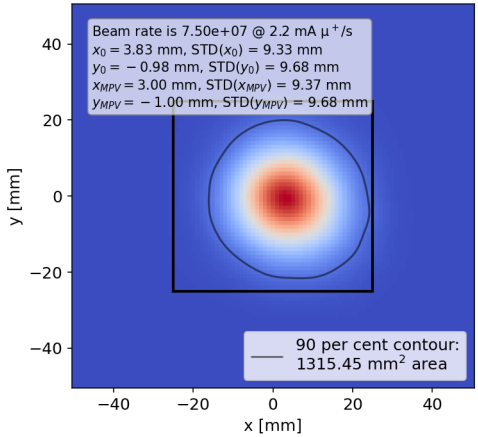

G4beamline transmission simulation

Surface muons transmission in the Mu3e spectrometer.

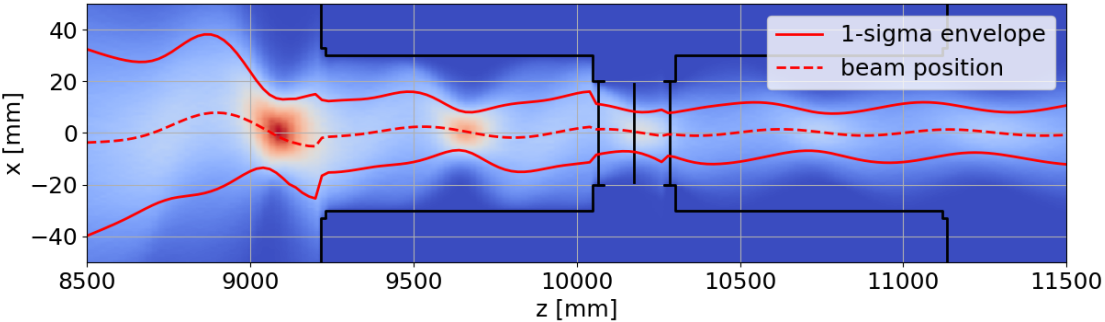

G4beamline transmission simulation

Surface muons transmission in the Mu3e spectrometer.

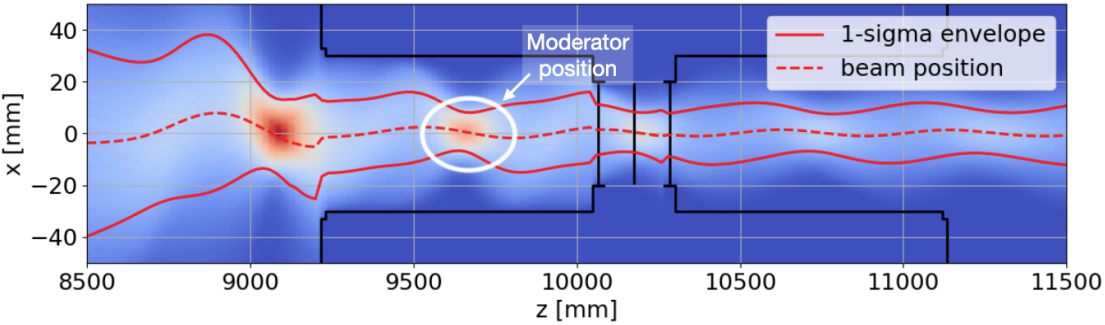

The HIMB project

Mu3e phase II

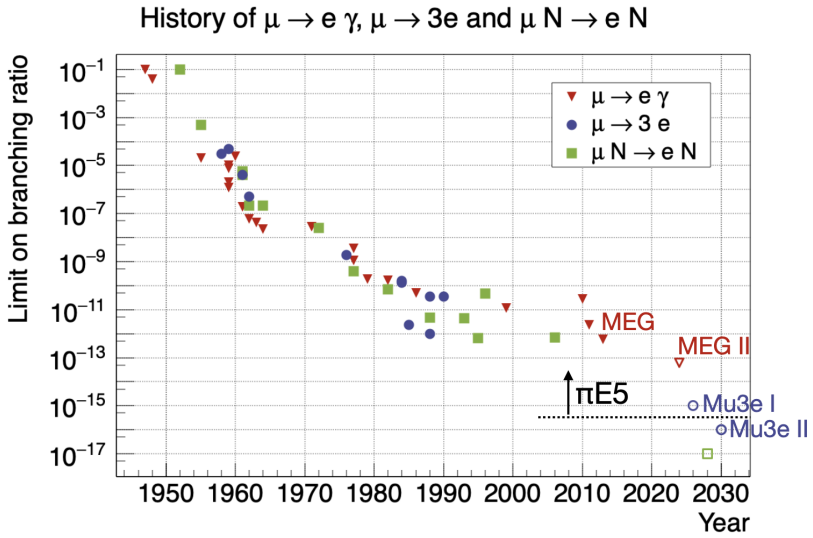

Mu3e phase II

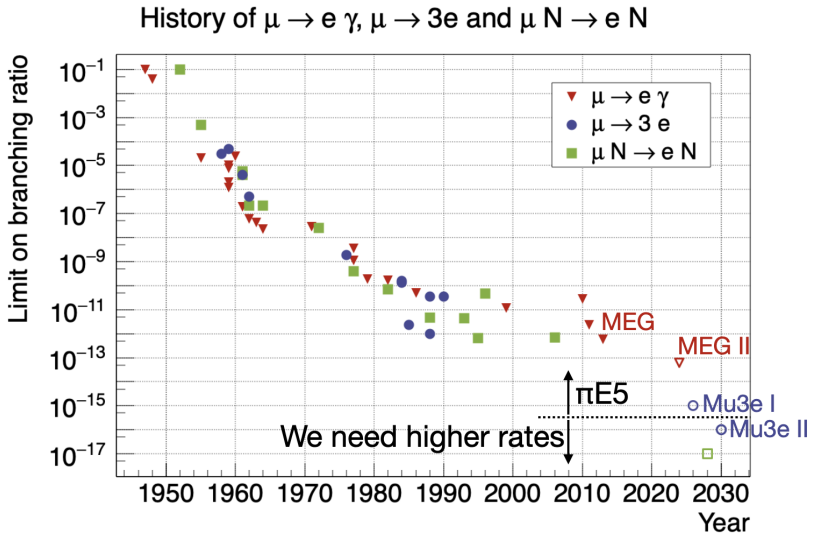

The High Intensity Muon Beams project

The High Intensity Muon Beams project aims to develop two new beamlines capable of delivering up to $10^{10}\ \mu^+/\mathrm{s}$.

There are two key points to do so:

- Substituting the old TgM station with a new version able to increase the particle production.
- Construction of two high capture/transport efficiency beamlines based on solenoids.

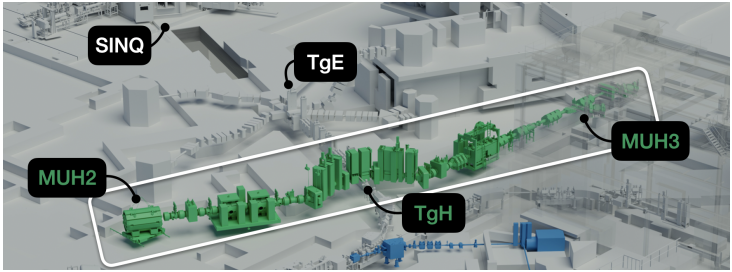

The High Intensity Muon Beams project

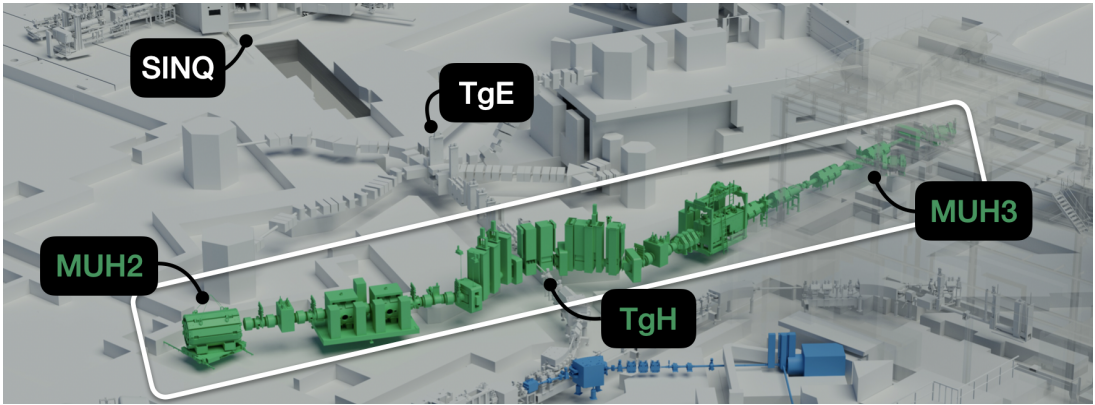

TgH: design

The plan is to substitute the existing Target M station with a high-intensity version using a slanted target geometry:

- thicker target
- slanting angle
- muon collection sideways

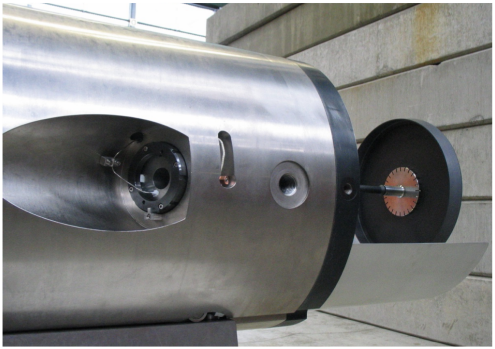

Existing TgM

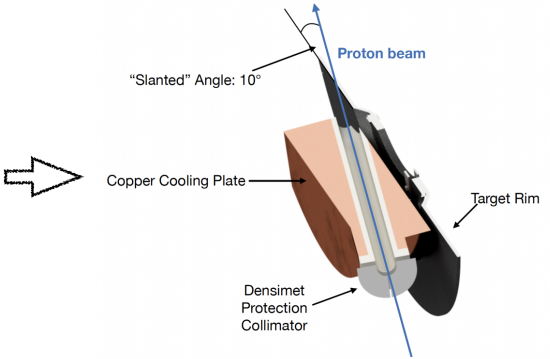

New TgH

Particle production at TgH

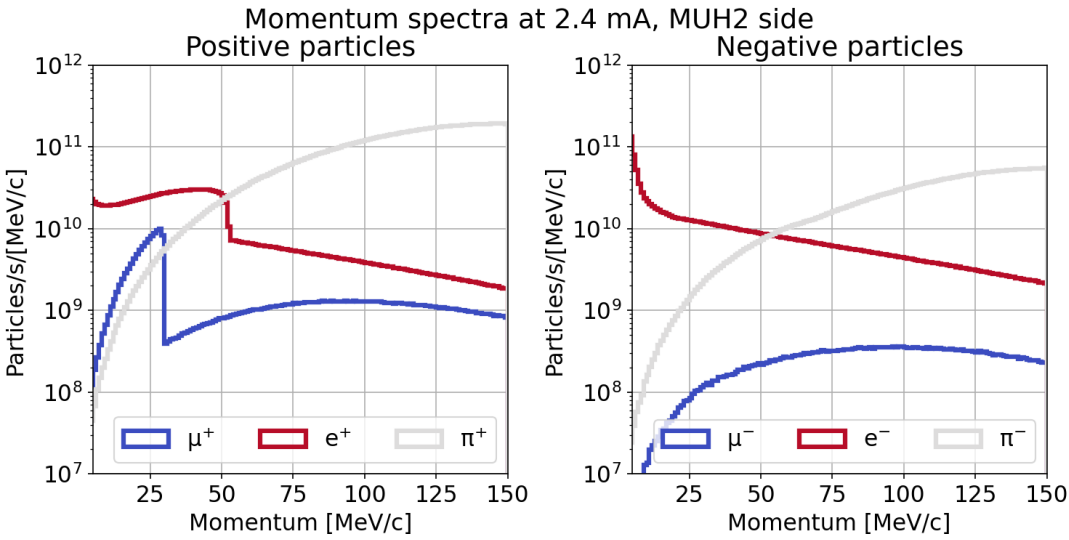

Particle production at TgH

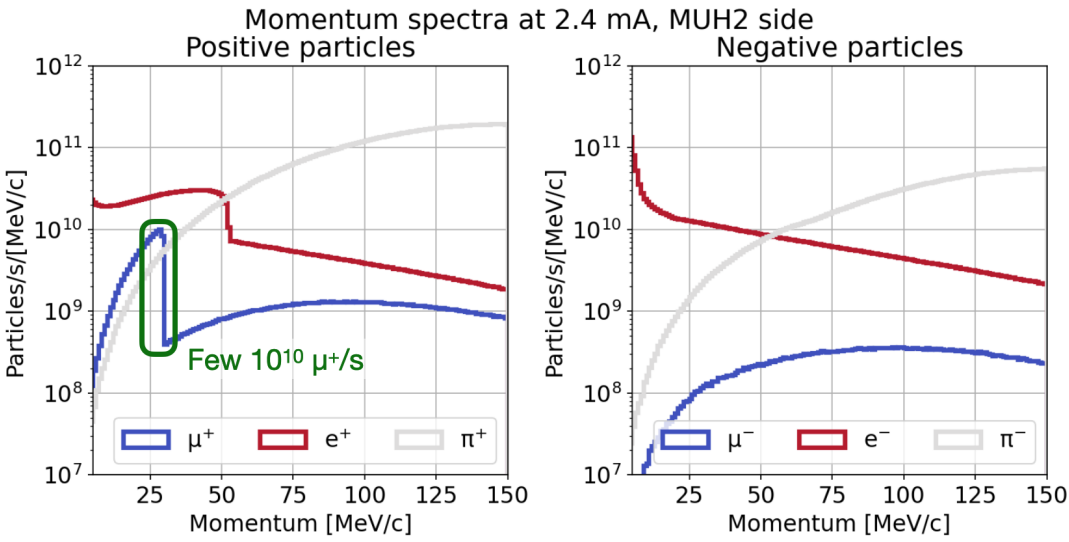

Particle production at TgH

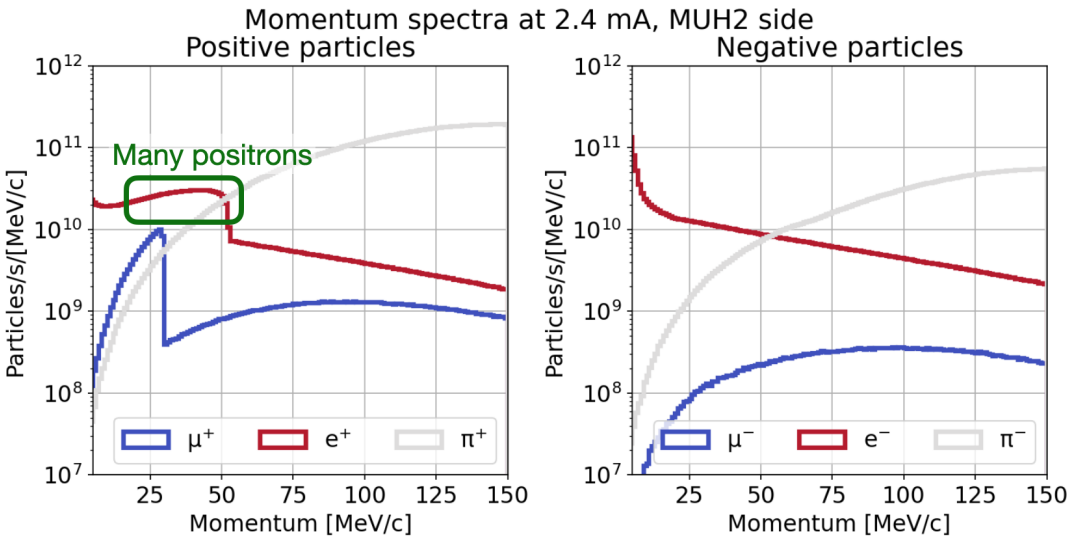

Particle production at TgH

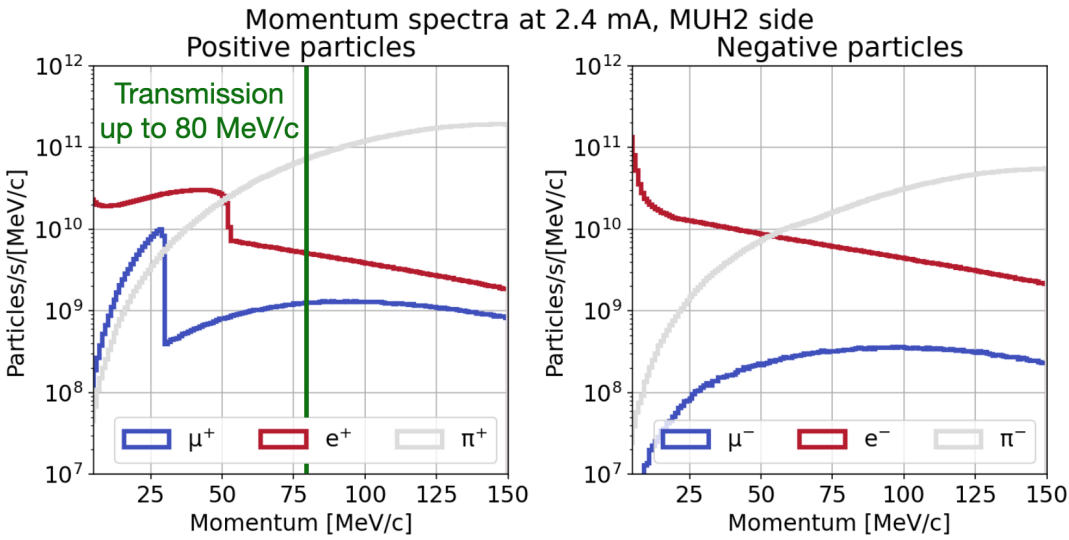

MUH2

Aimed at particle physics experiments, highest rates exceeding $10^{10}\,\mu^+/\mathrm{s}$.

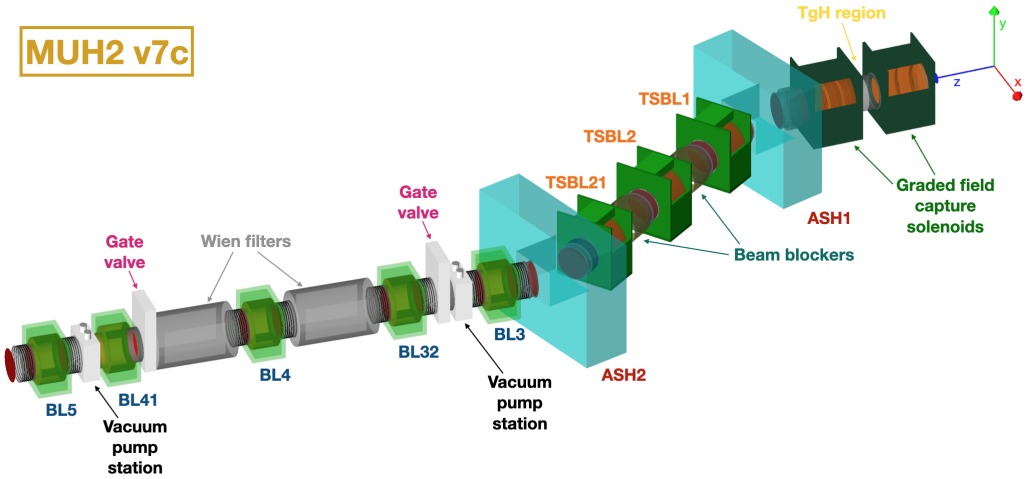

Optimization

Many optimizations/single particle tracking simulations (expensive) $\rightarrow$ **hyperparameter searches**.

Bayesian optimization:

- probabilistic approach to parameter space exploration, next trial to test is the best guess for the maximum
- $\mathcal{O}(10)$ parameters/one or many (multi) figures of merit

Genetic algorithms:

- evolutionary approach to function maximization, fittest individuals are used to produce the next generation
- $> \mathcal{O}(20)$ parameter/many figures of merit

Optimization

Bayesian optimization:

- probabilistic approach to parameter space exploration, next trial to test is the best guess for the maximum
- $\mathcal{O}(10)$ parameters/one or many (multi) figures of merit

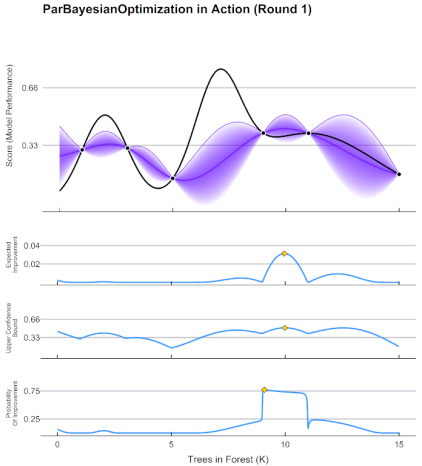

Optimization

Many optimizations/single particle tracking simulations (expensive) $\rightarrow$ **hyperparameter searches**.

Bayesian optimization:

- probabilistic approach to parameter space exploration, next trial to test is the best guess for the maximum
- $\mathcal{O}(10)$ parameters/one or many (multi) figures of merit

Genetic algorithms:

- evolutionary approach to function maximization, fittest individuals are used to produce the next generation
- $> \mathcal{O}(20)$ parameter/many figures of merit

Optimization

Many optimizations/single particle tracking simulations (expensive) $\rightarrow$ **hyperparameter searches**.

Bayesian optimization:

- probabilistic approach to parameter space exploration, next trial to test is the best guess for the maximum
- $\mathcal{O}(10)$ parameters/one or many (multi) figures of merit

Genetic algorithms:

- evolutionary approach to function maximization, fittest individuals are used to produce the next generation
- $> \mathcal{O}(20)$ parameter/many figures of merit

Bayesian vs genetic

21 free parameters are optimized here.

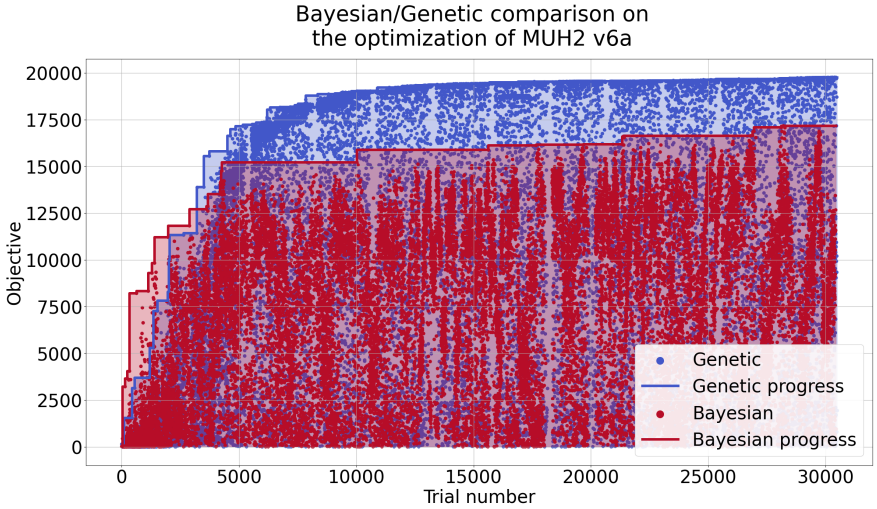

MUH2 deliverable rates

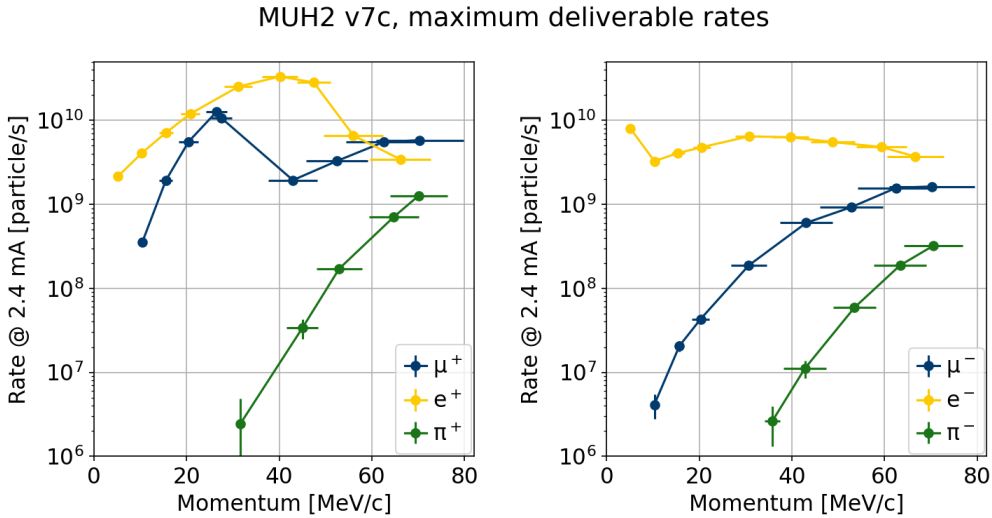

MUH2 beam spot optimization

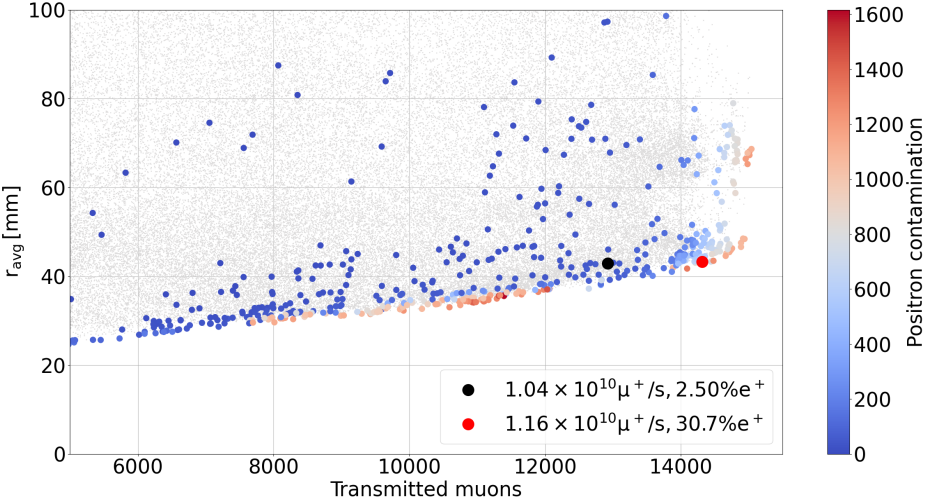

X17 analysis

The beryllium anomaly

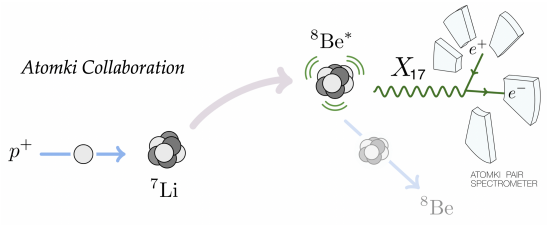

In 2016 the ATOMKI collaboration found an excess in the $^7\mathrm{Li}(\mathrm{p}, \mathrm{e}^+\mathrm{e}^-)^8\mathrm{Be}$ reaction: an excess of event is found in the internal pair conversion (IPC).

Excess was attributed to a light boson:

- $m_{X17} = 16.98\,\mathrm{MeV}/c^2$
- $\mathrm{BR}(X17/\gamma) = 6 \times 10^{-6}$

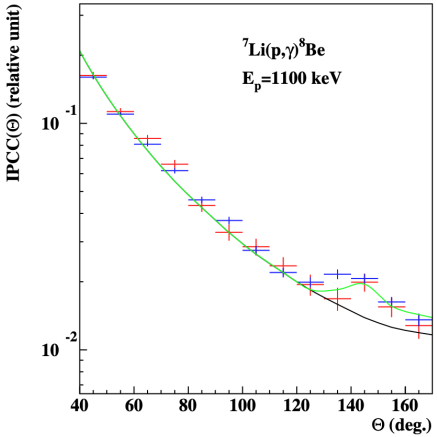

The beryllium anomaly

The anomaly was observed in the $1.03\,\mathrm{MeV}$ resonance.

Additionally it was observed by ATOMKI in the $^{3}\mathrm{H}(\mathrm{p},\mathrm{e}^{+}\mathrm{e}^{-})^{4}\mathrm{He}$ process and in the $^{11}\mathrm{B}(\mathrm{p},\mathrm{e}^{+}\mathrm{e}^{-})^{12}\mathrm{C}$ process.

All measurements were performed with the same detection scheme in the plane perpendicular to the proton beam.

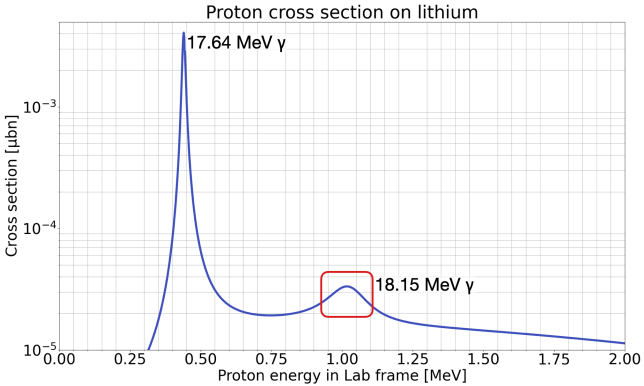

The beryllium anomaly

The anomaly was observed in the $1.03\,\mathrm{MeV}$ resonance.

Additionally it was observed by ATOMKI in the $^{3}\mathrm{H}(\mathrm{p},\mathrm{e}^{+}\mathrm{e}^{-})^{4}\mathrm{He}$ process and in the $^{11}\mathrm{B}(\mathrm{p},\mathrm{e}^{+}\mathrm{e}^{-})^{12}\mathrm{C}$ process.

All measurements were performed with the same detection scheme in the plane perpendicular to the proton beam.

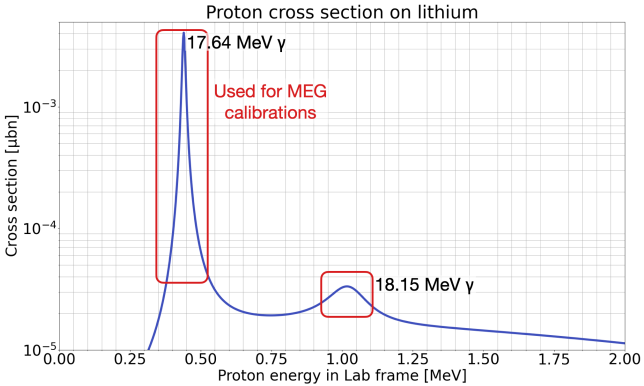

The beryllium anomaly

The anomaly was observed in the $1.03\,\mathrm{MeV}$ resonance.

Additionally it was observed by ATOMKI in the $^{3}\mathrm{H}(\mathrm{p},\mathrm{e}^{+}\mathrm{e}^{-})^{4}\mathrm{He}$ process and in the $^{11}\mathrm{B}(\mathrm{p},\mathrm{e}^{+}\mathrm{e}^{-})^{12}\mathrm{C}$ process.

All measurements were performed with the same detection scheme in the plane perpendicular to the proton beam.
→ **Among other efforts, MEG II can provide an independent test in a wider angular acceptance.**

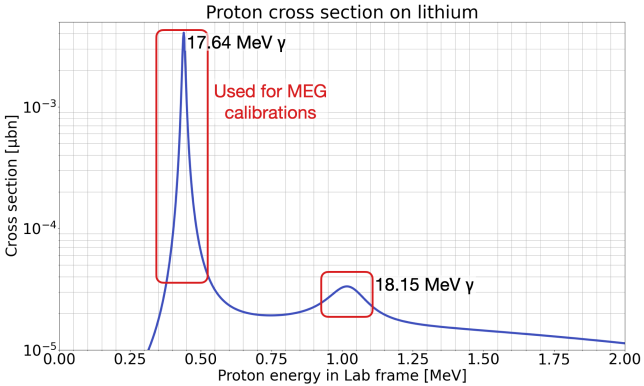

MEG II detector

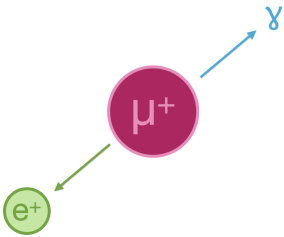

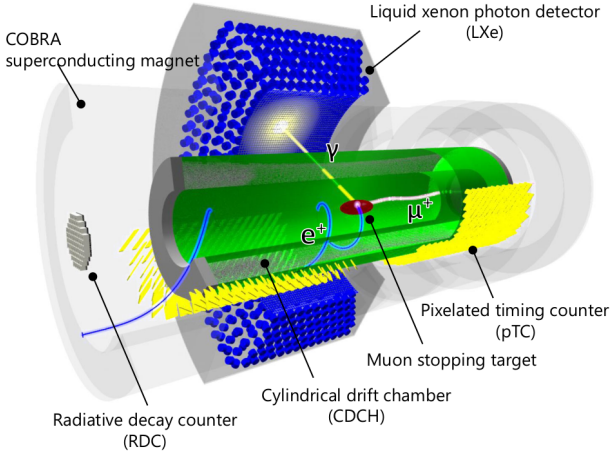

MEG II detector

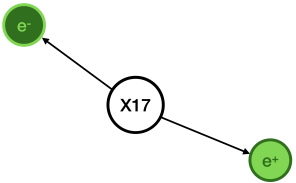

- angular aperture of the pair
- rest mass of the pair
- timing

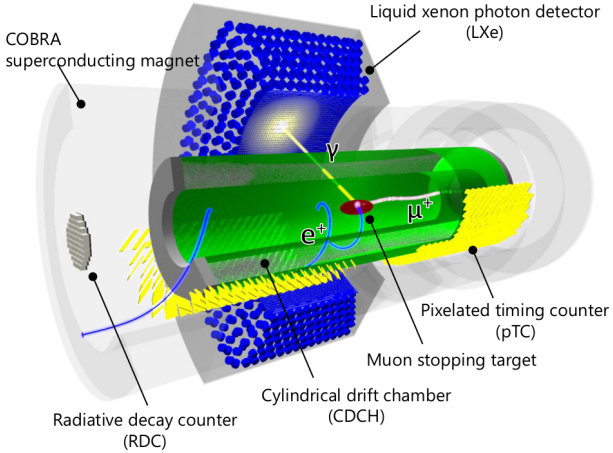

MEG II detector

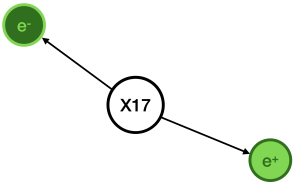

- **angular aperture of the pair**
- **rest mass of the pair**
- timing

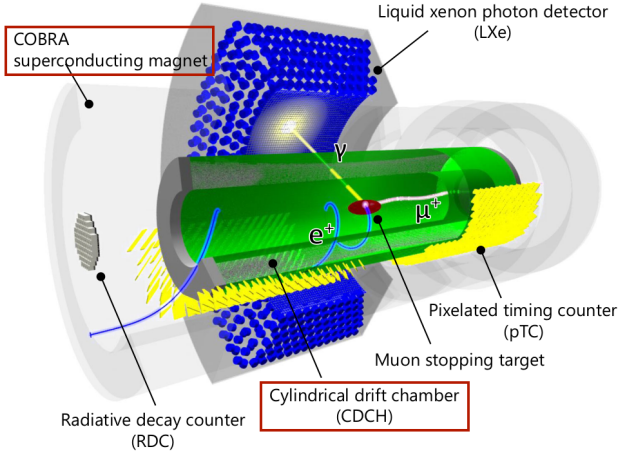

MEG II detector

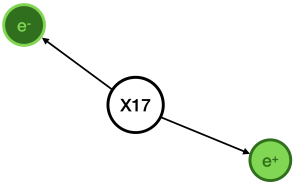

- angular aperture of the pair
- rest mass of the pair
- **timing**

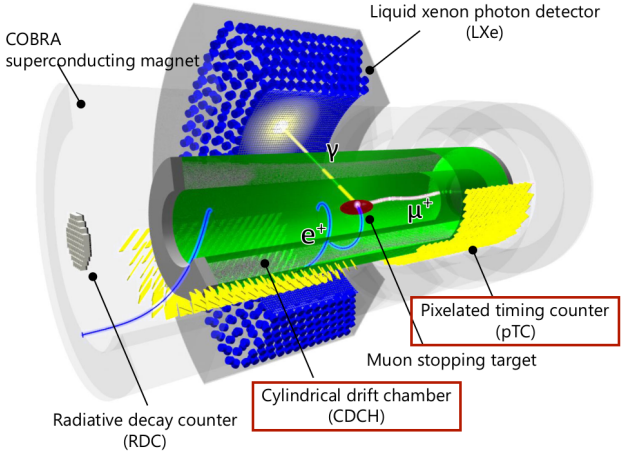

MEG II detector

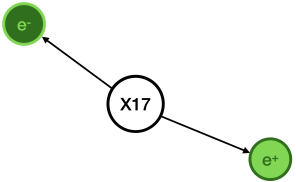

- angular aperture of the pair
- rest mass of the pair
- timing
- **lithium target (**$2\,\mu m$**)**

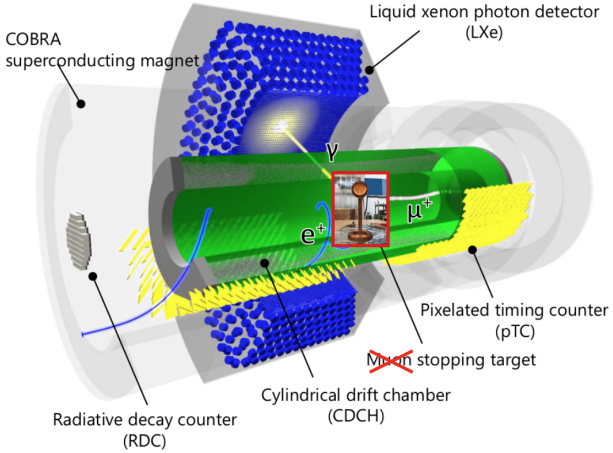

MEG II detector

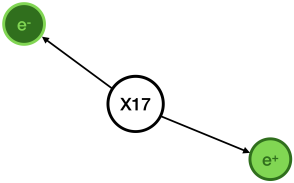

- angular aperture of the pair
- rest mass of the pair
- timing
- lithium target (2 µm)
- 1 MeV **proton beam**

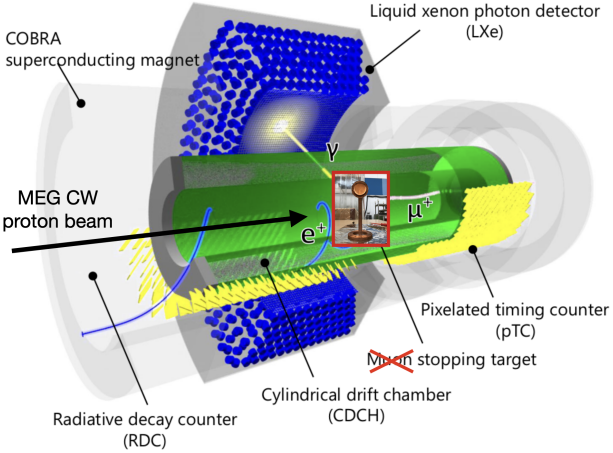

Backgrounds

The main backgrounds are:

- internal pair creation (IPC)
- external pair creation (EPC)

Both processes occur in the $15\,\text{MeV}$ and $18\,\text{MeV}$ lines.

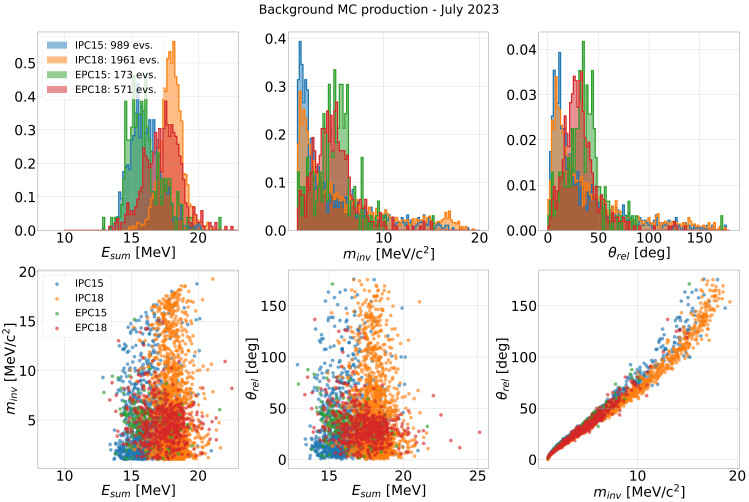

Backgrounds

The main backgrounds are:

- internal pair creation (IPC)
- external pair creation (EPC)

Both processes occur in the $15\,\text{MeV}$ and $18\,\text{MeV}$ lines.

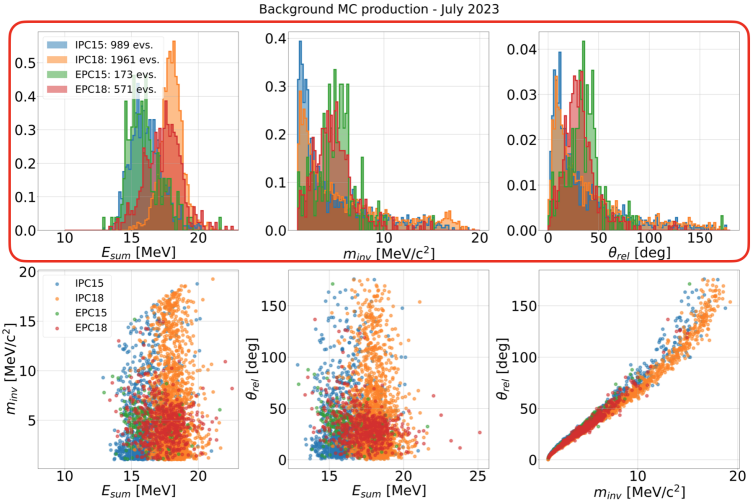

Backgrounds

The main backgrounds are:

- internal pair creation (IPC)
- external pair creation (EPC)

Both processes occur in the $15\,\text{MeV}$ and $18\,\text{MeV}$ lines.

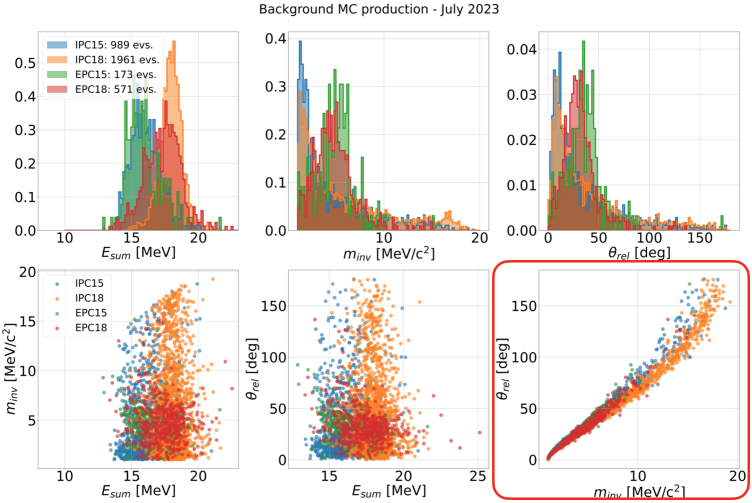

Backgrounds

The main backgrounds are:

- internal pair creation (IPC)
- external pair creation (EPC)

Both processes occur in the $15\,\text{MeV}$ and $18\,\text{MeV}$ lines.

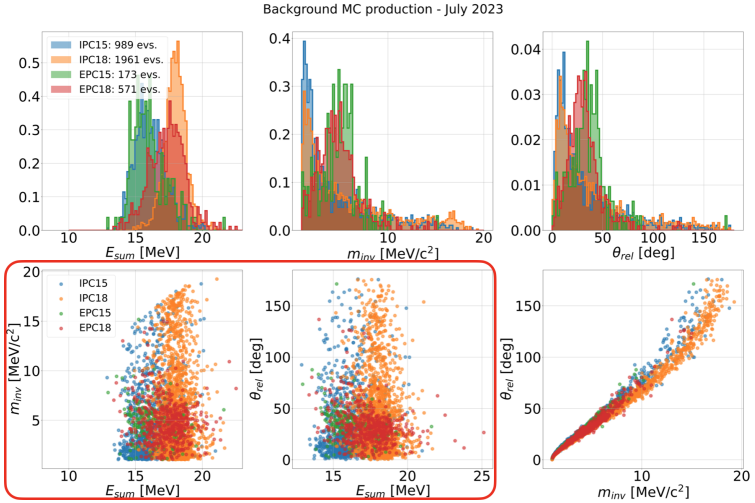

2023 data - blinding

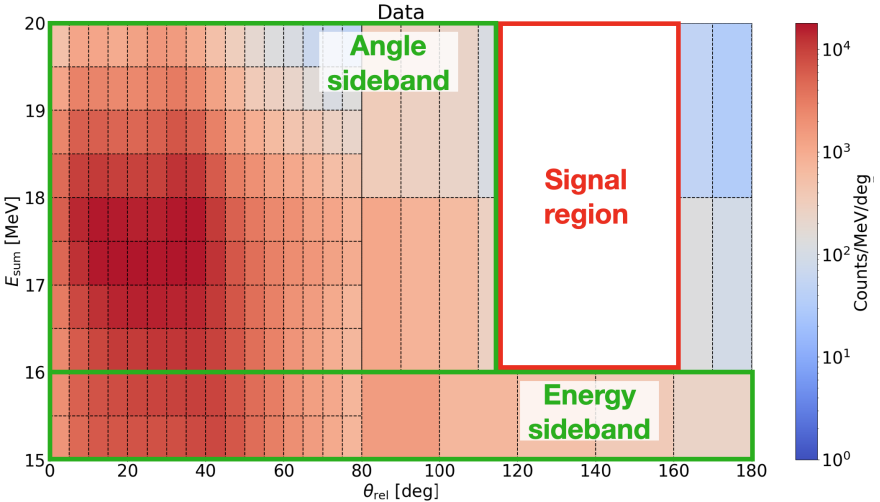

Figure: 2023 data

Likelihood analysis

The background and the signal PDFs are modeled with histograms (templates) from the MC production.

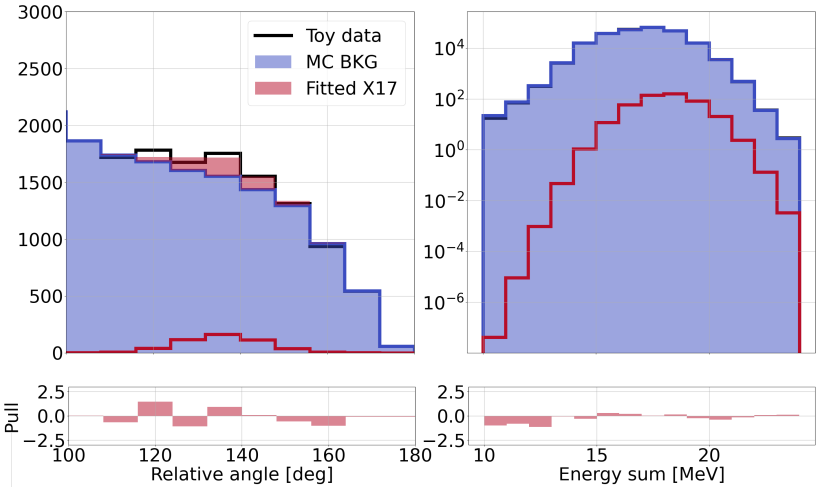

Sensitivity estimate

The $90\,\%$ CL bands on X17 yield and mass are computed with the Feldman-Cousins prescription. Due to the low expected EPC MC statistics, the expected sensitivity was computed for two different scenarios:

- *ideal statistics*: $\sim 10^5$ events produced
- *realistic statistics*: $\sim 10^4$ events produced

$\mathcal{N}_{\mathrm{X17}}(\mathcal{B})$	0 (0)		450 (6×10^{-6})	
Scenario	$90\,\%$ LL	$90\,\%$ UL	$90\,\%$ LL	$90\,\%$ UL
Ideal	-	275 (3.7×10^{-6})	271 (3.6×10^{-6})	657 (8.8×10^{-6})
Realistic	-	272 (3.6×10^{-6})	215 (2.9×10^{-6})	638 (8.5×10^{-6})

Target condition in 2023

The shown sensitivities are expected for a pure 1.03 MeV resonance. We found that the target used in 2023 is thicker than expected, meaning the 441 keV resonance is dominant.

No major changes are expected in the sensitivity.

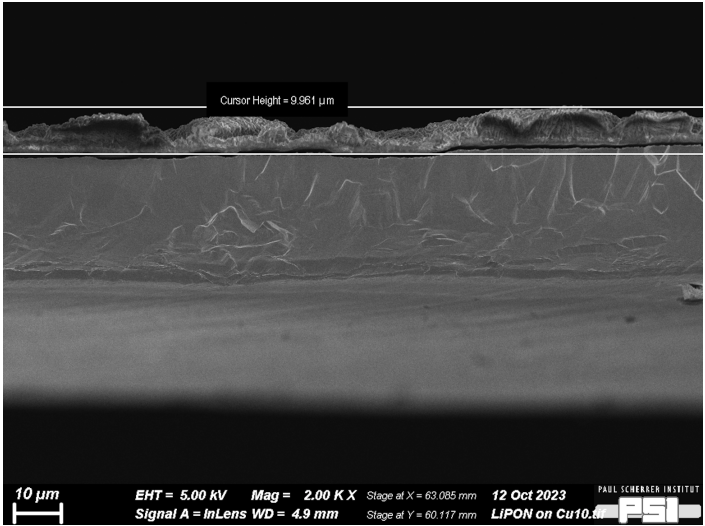

Conclusions and outlook

- The commissioning of the CMBL was completed with a maximum muon rate of $7.5 \times 10^7\ \mu^+/\mathrm{s}$ at the position of the Mu3e target. The beamline is ready for data taking.
- The current designs of the HIMB beamlines are expected to deliver the desired rates of $10^{10}\ \mu^+/\mathrm{s}$. We expect to publish a TDR by the end of 2024 and do the upgrade in 2027/2028.
- The framework for the likelihood analysis of the X17 was adapted for template fits. We expect to unblind in the next weeks and improve the target for another data taking run at the end of 2024.

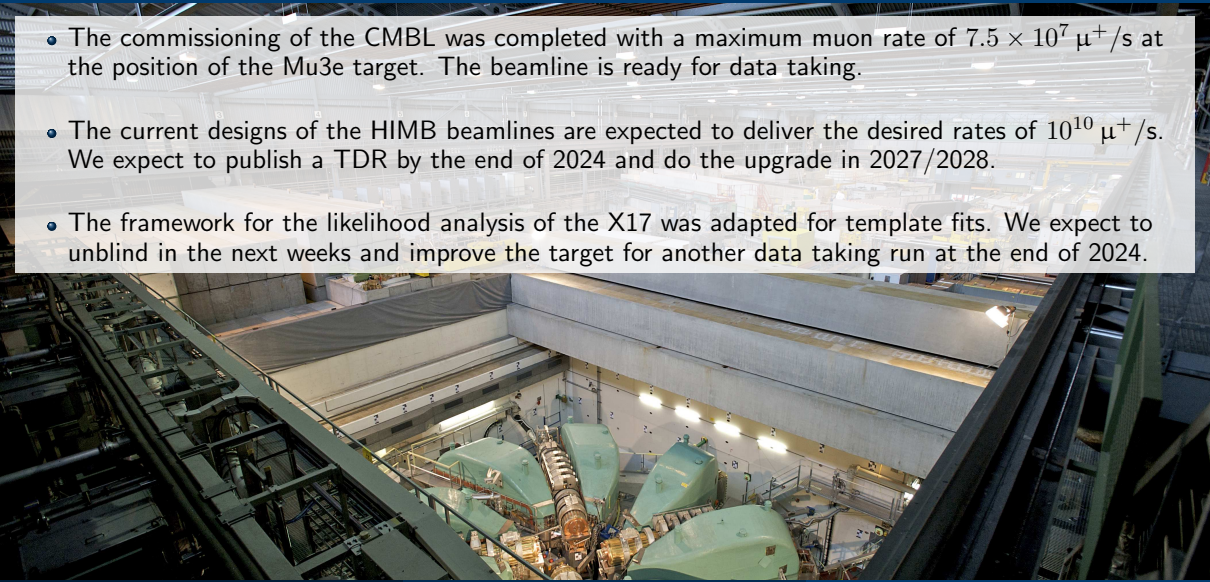

Lectures and teaching

Courses for PhD credits at ETH Zürich:

- autumn 2021:
  - "Learning to Teach": this course imparted a variety of teaching skills that help Doctoral Teaching Assistants with their teaching tasks
  - "Astronomical Observations and Instrumentations": course focused on the main and recent astronomical observations and description of the most relevant employed instrumentations
- spring 2022:
  - Joint Universities Accelerator School, COURSE 2: technology and applications of particle accelerators
- summer 2022:
  - Engaging Physics Tutoring Summer Camp
  - PSI Particle Physics Summer School - Vision and Precision
- autumn 2022:
  - Pluralist Philosophy of Mathematics: the goal is to introduce students to mainstream philosophies of mathematics.

Teaching at ETH Zürich:

- autumn 2021: Physics 1 exercise class for Medicine and Health Sciences students
- spring 2022: Physics 2 exercise class for Medicine and Health Sciences students
- autumn 2022: Physics 1 Übungschef for Medicine and Health Sciences students
- spring 2023: Physics 2 Übungschef for Medicine and Health Sciences students

Conferences

Training:

- 20-21 May 2021: *First Muon Community Meeting* (Muon Collider Workshop), Online
- 2-4 August 2021: *Fermilab 2021 Summer Student School at LNF*, Laboratori Nazionali di Frascati INFN Online
- 6-8 September 2021: *Shedding light on X17*, Centro Ricerche Enrico Fermi, Rome Online
- 24-26 November 2021: *International Workshop on Cosmic-Ray Muography (Muography2021)*, Ghent Online
- 4-6 July 2022: *LF(U)V Workshop*, Universität Zürich.

Conferences and workshops:

- 6-9 April 2021: *HIMB Physics Case Workshop*, PSI - Paul Scherrer Institut Online
- 10-11 June 2021: *CHIPP Plenary 2021*, Spiez Switzerland. Poster:"High Intensity Muon Beam project(HIMB): how to improve the most intense muon beam in the world"
- 30 August-3 September 2021: *Joint Annual Meeting of the APS SPS*, Universität Innsbruck. Talk: "High Intensity Muon Beam project (HIMB): how to improve the most intense muon beam in the world"
- 22-28 May 2022: *Pisa Meeting on Advanced Detectors - Edition 2022*, La Biodola - Isola d'Elba, Italy. Poster: "Beam monitoring detectors for High Intensity Muon Beams" + proceedings
- 27-30 June 2022: *Annual Meeting of the Swiss Physical Society*, Université de Fribourg. Talk: "High Intensity Muon Beam (HIMB): how to improve the most intense muon beam in the world"
- 29 August - 2 September 2022: *8th International Symposium on Symmetries in Subatomic Physics*, Universität Wien. Invited talk + proceedings: "Future facilities at PSI, the High-Intensity Muon Beams (HIMB) project".
- 16-21 October 2022: *Physics of fundamental Symmetries and Interactions - PSI2022*, Paul Scherrer Institut. Poster: "Multi-Objective Genetic Optimization for the High-Intensity Muon Beams at PSI".
- 15-17 February 2023: *New Physics Signals 2023 - NePsi 2023*, Department of Physics, Pisa University. Poster: "Multi-Objective Genetic Optimization for the High-Intensity Muon Beams at PSI".

Publications and secondments

Publications:

- A. Baldini et al., "The Search for $\mu^+ \to e^+\gamma$ with 10–14 Sensitivity: The Upgrade of the MEG Experiment", Symmetry 2021, 13(9), 1591 (https://doi.org/10.3390/sym13091591);
- M. Aiba et al., "Science Case for the new High-Intensity Muon Beams HIMB at PSI", arXiv:2111.05788.
- Eichler, R. et al. "IMPACT conceptual design report", (PSI Bericht, Report No.: 22-01). Paul Scherrer Institut.
- G. Dal Maso et al., "Beam monitoring detectors for High Intensity Muon Beams", Nucl. Instrum. Methods A (https://doi.org/10.1016/j.nima.2022.167739)
- G. Dal Maso et al., "Future facilities at PSI, the High-Intensity Muon Beams (HIMB) project", EPJ Web of conferences, (https://doi.org/10.1051/epjconf/202328201012)

Secondments:

- secondment at University of Tokyo for X17 analysis, 13th March - 5th April 2023
- secondment at University of Pisa for X17 analysis, 11th-28th April 2023

Back-up

Charged Lepton Flavor Violation

cLFV is possible in the SM, but not observable:

$$\mathcal{B}_{SM} \propto \left(\frac{\Delta m_\nu^2}{m_W^2}\right)^2 \simeq 10^{-54}$$

The observation of a SM prohibited decay would give hint of BSM physics:

$$\mathcal{B}_{BSM} \propto \frac{1}{\Lambda^4}$$

At PSI two experiments measure such golden channels: MEG II and Mu3e.

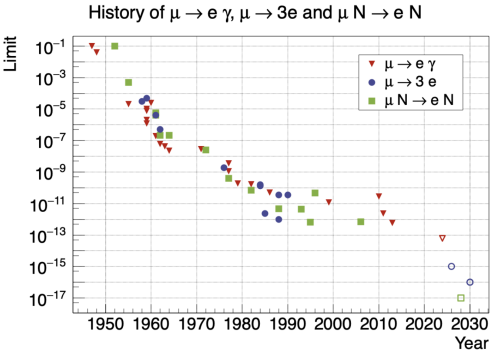

Mu3e detector

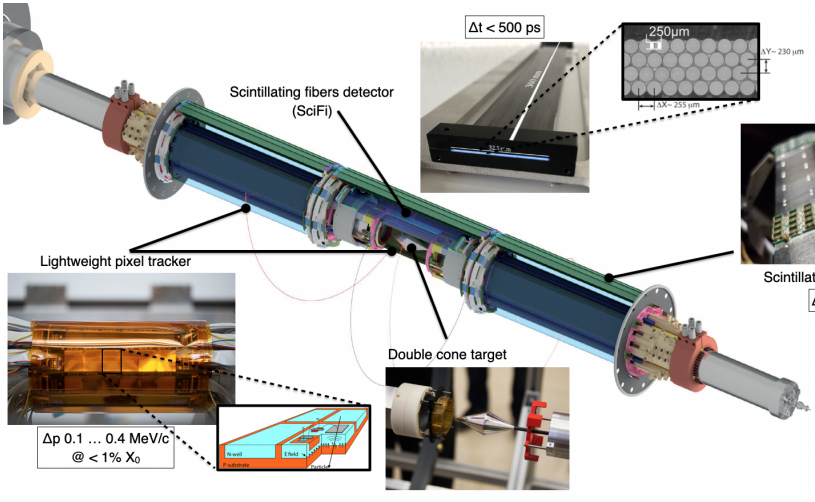

Quadrupole scan

In practice, one can express the beam width with the matrix formalism. In πE5 we use the QSK43 quadrupole for such measurement:

$$M(s_0|s) = M_{\text{drift}}(s_1|s) M_{\text{QSK43}}(s_2|s_1) M^{-1}_{\text{QSK43,opt}}(s_1|s_2) M^{-1}_{\text{drift}}(s_1|s_0) \tag{1}$$

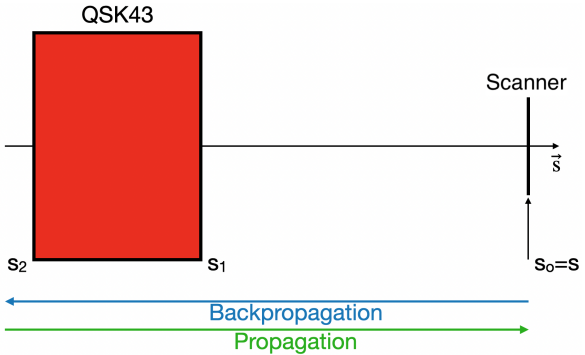

Quadrupole scan

This is a measurement we performed in June 2022 in πE5.
We must keep in mind that: **we are assuming a gaussian beam** and that this measurement depends on our knowledge of the quadrupole magnet.

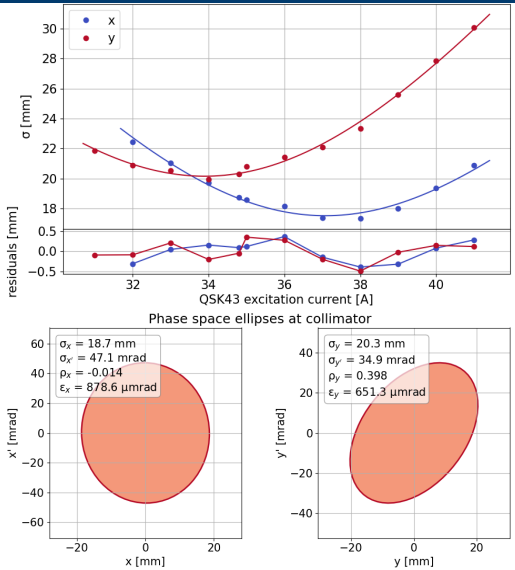

Single-slit measurement

A common approach to measure the emittance of low energy proton beams is to measure the beam spot in presence of an adjustable silts system with a small aperture.

- the slits are thick enough to dump the beam
- the aperture is small enough to consider the resulting beamlet as coming from a point-like source
- after a drift the beamlet is measured and its profile is proportional to the divergence at the aperture location

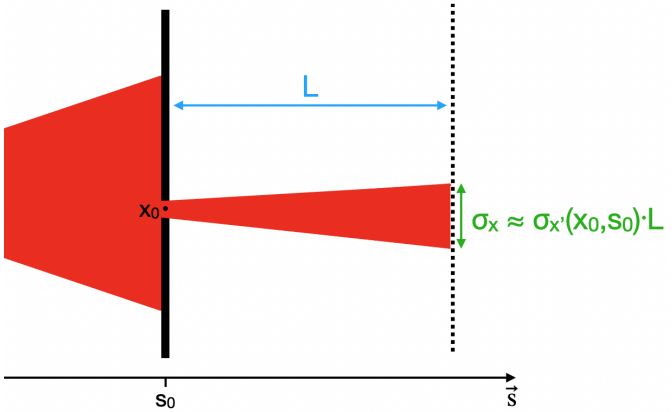

Pepper-pot measurement

The scan was performed on the horizontal and vertical axes with an $0.5\,\text{mm}$ pitch. The area filled in the plots below are the measured background.

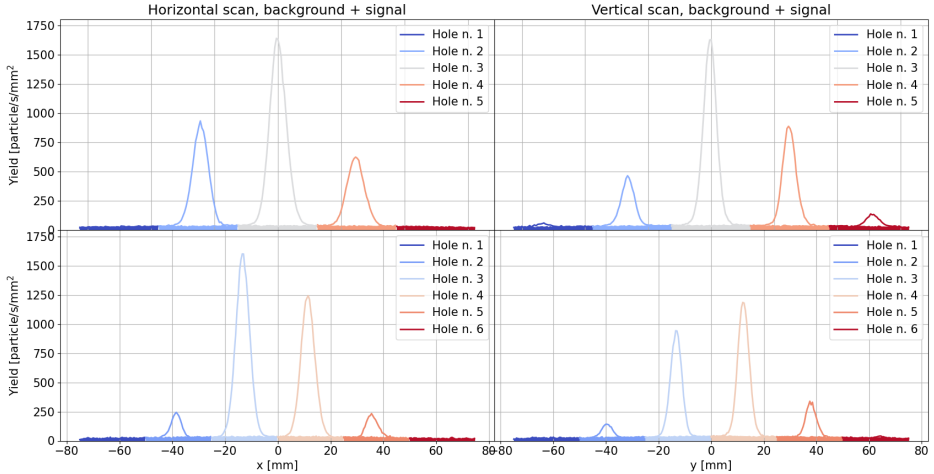

MCS effect

In case of a pepper-pot scan, the beamlets profiles are proportional to the divergence distribution at the plate location:

1. each beamlet is expected to be broadened by MCS the same way as the divergence is increased up to the plate
2. after the plate each beamlet will increase in size as in the quadrupole case
3. each beamlet is expected to be displaced depending on the hole position

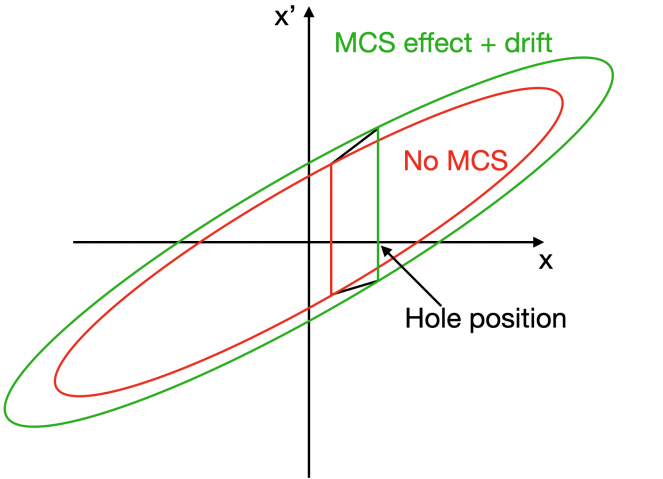

Pepper-pot measurement results

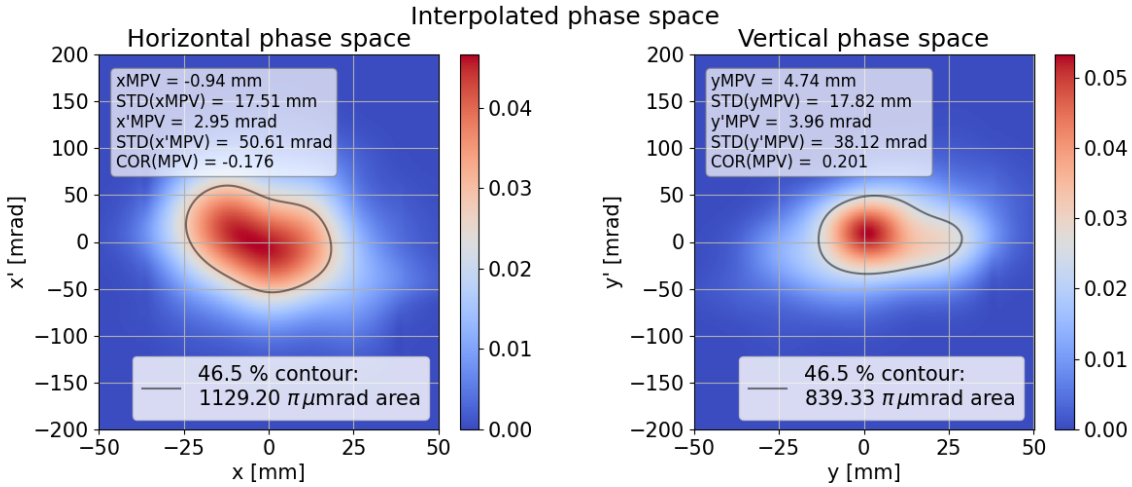

Beam spot at moderator/collimator position

We first removed a piece of the large beam pipe, 400 mm long, to measure the beam, without insert, where the moderator/collimator should be to check that we have a focus.

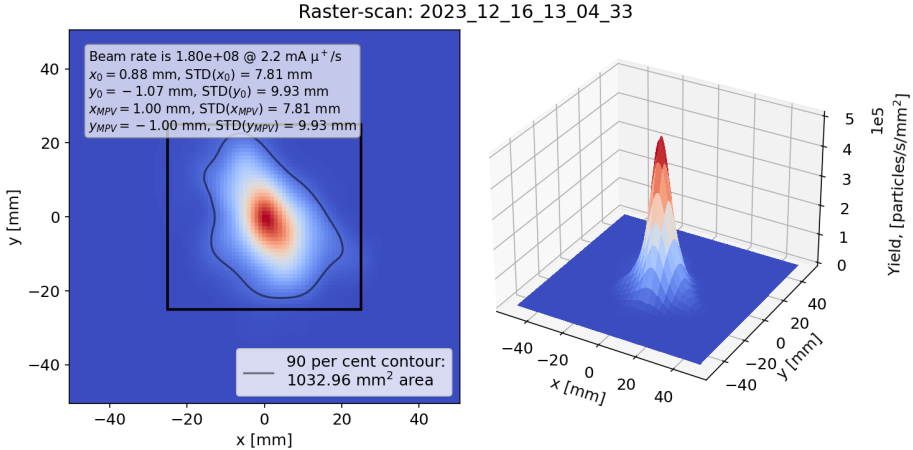

Beamline status and results

CMBL commissioning rates comparison			
	Rate [μ^+/s] @ 2.2 mA		
Year	Collimator	QSM41	Mu3e
2021	1.94 10^8	1.10 10^8	4.40 10^7
2022	2.26 10^8	1.66 10^8	6.89 10^7
2023	2.38 10^8	1.88 10^8	7.50 10^7*
TDR	-	-	6-7 10^7

Table: In 2023 (*), the measurement at Mu3e center was performed with the moderator in place.

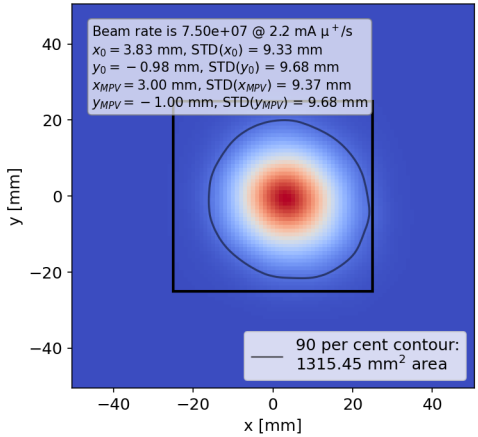

MEG II detector

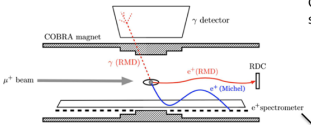

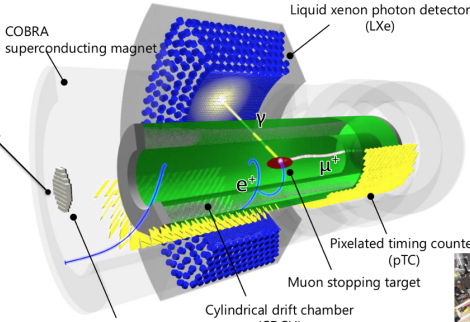

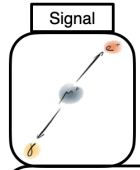

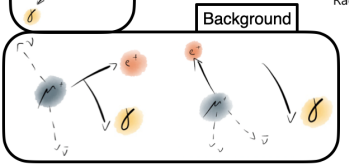

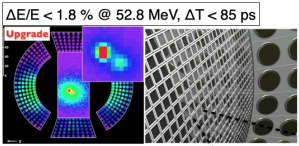

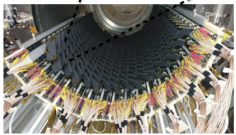

Δt < 35 ps

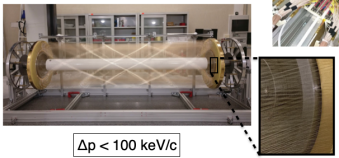

Δp < 100 keV/c

Science Case Workshop

We had a science case workshop between 6-9 April 2021.

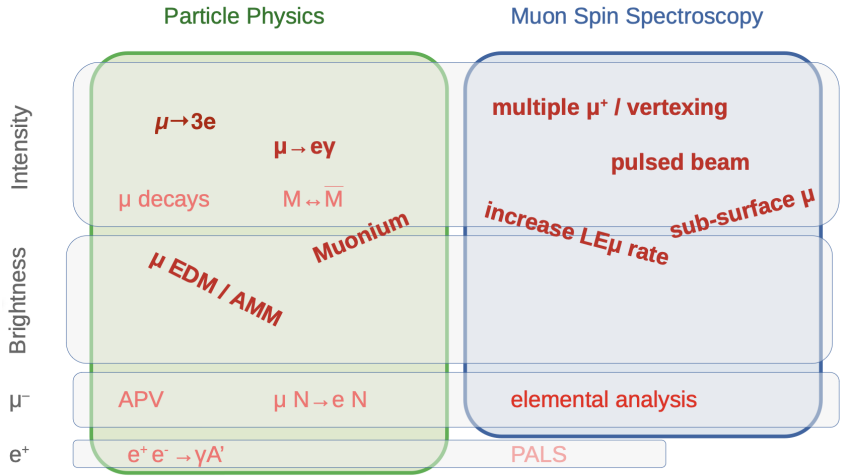

https://indico.psi.ch/e/himbws

Bayesian optimization

A Bayesian optimizer is a "black-box" global maximum/minimum finder.

At each iteration the parameters to be tested are updated based on the previous results: a posterior function is updated at every trial and maximized.

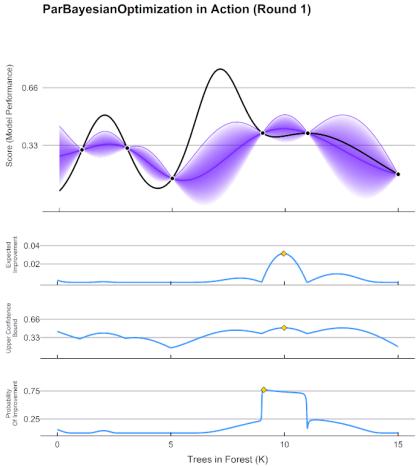

Non-dominated Sorting Genetic Algorithm-II

The basic idea is to define a population where each individual is characterized by his genes, namely the parameters of the problem.

At each epoch the individuals mix through breeding, crossover, mutation ...

The population is classified based on dominance and crowding distance.

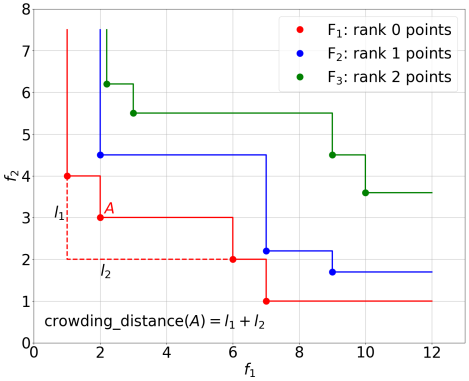

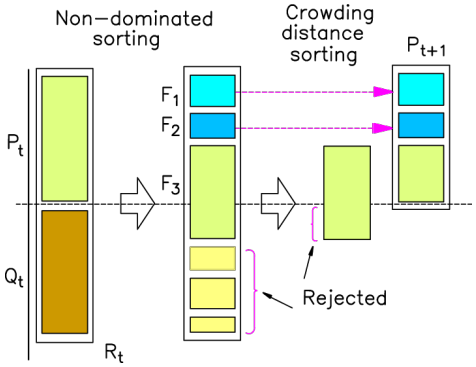

TargetH station

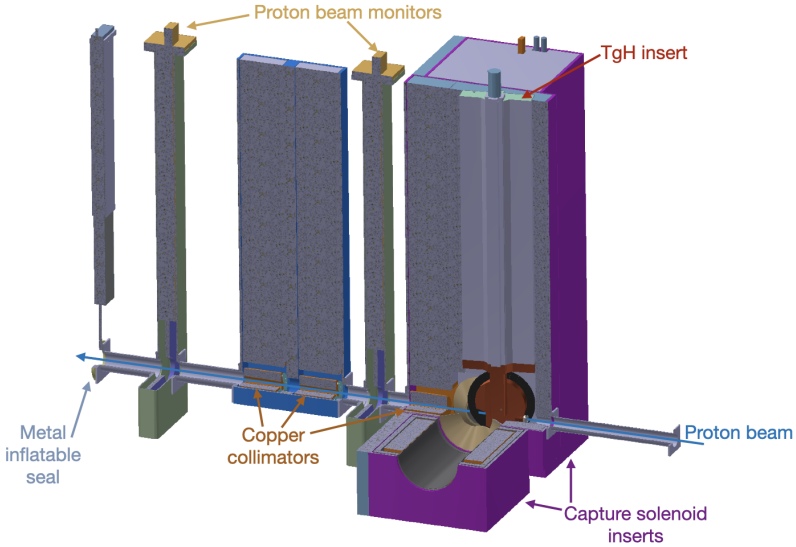

Graded field capture solenoids

The capture is performed with two normal conducting solenoids. The coils are grouped in three sets to be energized independently, allowing for:

- strong field close to the target → increased capture
- lower field for focusing DS → increased transmission

27 % **absolute rate increase w.r.t previous design.**

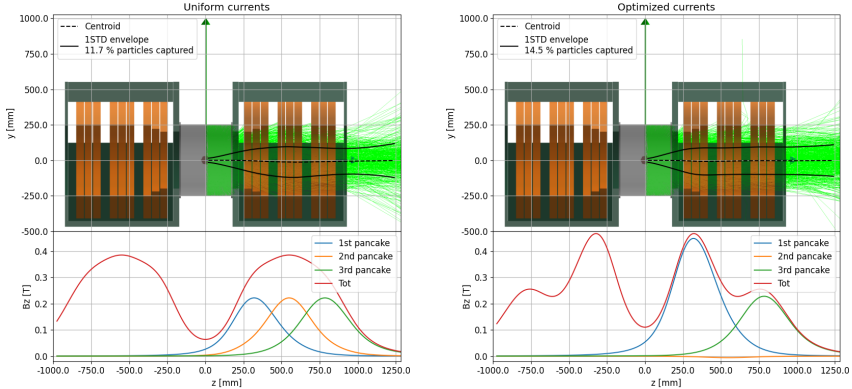

MUH2 envelope

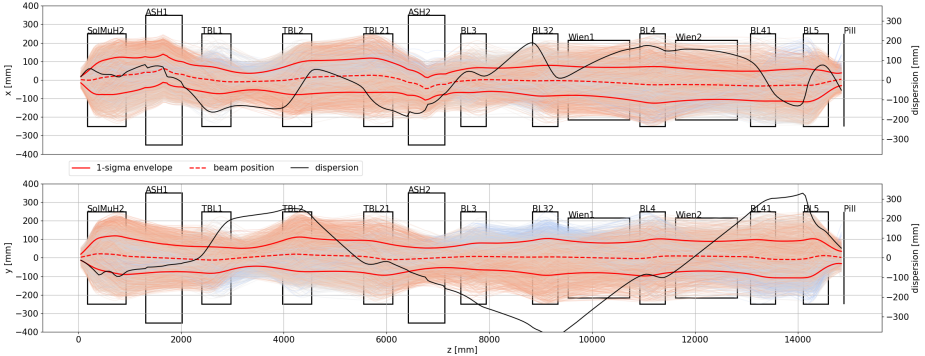

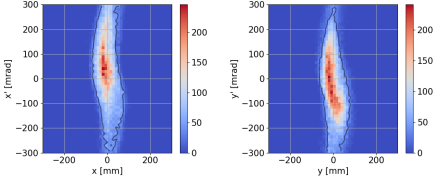

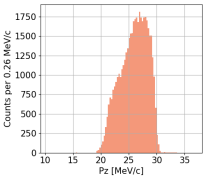

Rate @ 2.4 mA: 1.00e+10 μ^+/s
$x_{avg} = 3.62$ mm
STD(x_{avg}) = 34.21 mm
$xp_{avg} = 49.92$ mrad
STD(xp_{avg}) = 179.10 mrad
$y_{avg} = 1.85$ mm
STD(y_{avg}) = 33.12 mm
$yp_{avg} = -41.39$ mrad
STD(yp_{avg}) = 180.95 mrad
$\varepsilon_{x,\ 90\%} = 17.83\pi$ mm mrad
$\varepsilon_{y,\ 90\%} = 16.03\pi$ mm mrad
$P_{z,\ avg} = 25.69$ MeV/c
STD($P_{z,\ avg}$) = 2.37 MeV/c

MUH2 contamination

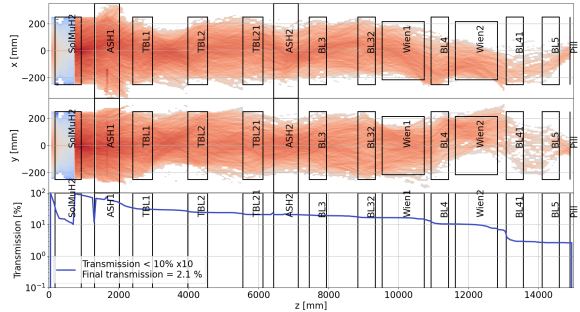

(a) Beam spot tune

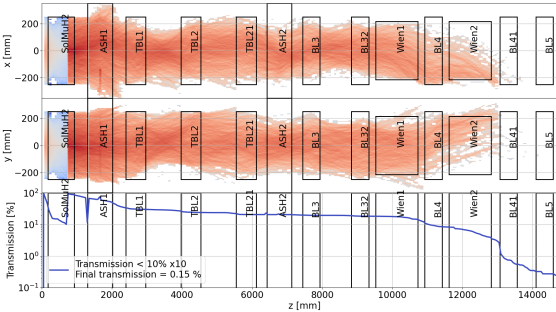

(b) Beam spot tune + contamination cut

MUH3 rates

Maximum deliverable rates after SpinRot1.

The DS settings can be found for surface muons and then matched for higher momenta.

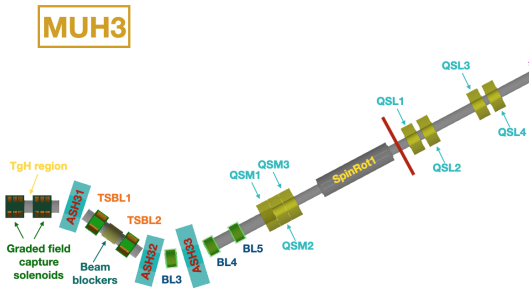

MUH3 v6, maximum muon rate tunes

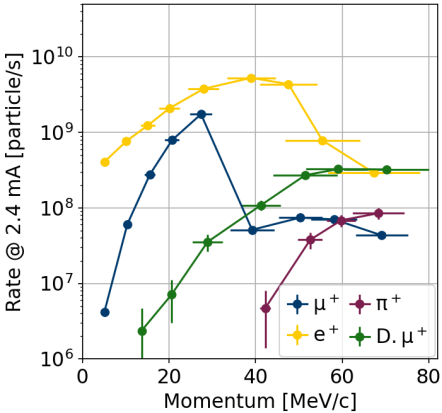

MUH3 matching

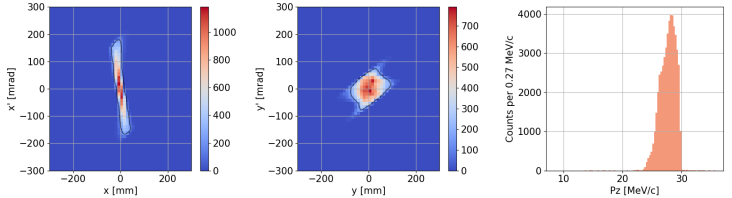

Rate @ 2.4 mA: 1.05e+09 μ^+/s
$x_{avg} = 0.24$ mm
STD(x_{avg}) = 15.83 mm
$xp_{avg} = 7.63$ mrad
STD(xp_{avg}) = 91.50 mrad
$y_{avg} = 2.84$ mm
STD(y_{avg}) = 38.28 mm
$yp_{avg} = 1.34$ mrad
STD(yp_{avg}) = 33.05 mrad
$\varepsilon_{x,90\%} = 3.99\pi$ rad mm
$\varepsilon_{y,90\%} = 4.54\pi$ rad mm
$P_{z,avg} = 27.50$ MeV/c
STD($P_{z,avg}$) = 1.36 MeV/c

(a) 27 MeV

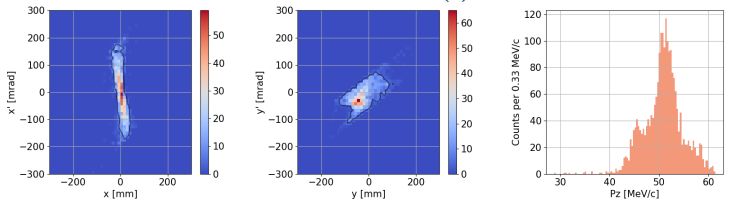

Rate @ 2.4 mA: 4.72e+07 μ^+/s
$x_{avg} = 3.21$ mm
STD(x_{avg}) = 16.99 mm
$xp_{avg} = 1.27$ mrad
STD(xp_{avg}) = 89.36 mrad
$y_{avg} = -22.01$ mm
STD(y_{avg}) = 48.31 mm
$yp_{avg} = -11.67$ mrad
STD(yp_{avg}) = 40.17 mrad
$\varepsilon_{x,90\%} = 4.42\pi$ rad mm
$\varepsilon_{y,90\%} = 5.52\pi$ rad mm
$P_{z,avg} = 50.74$ MeV/c
STD($P_{z,avg}$) = 3.79 MeV/c

(b) 50 MeV

MUH3 envelope

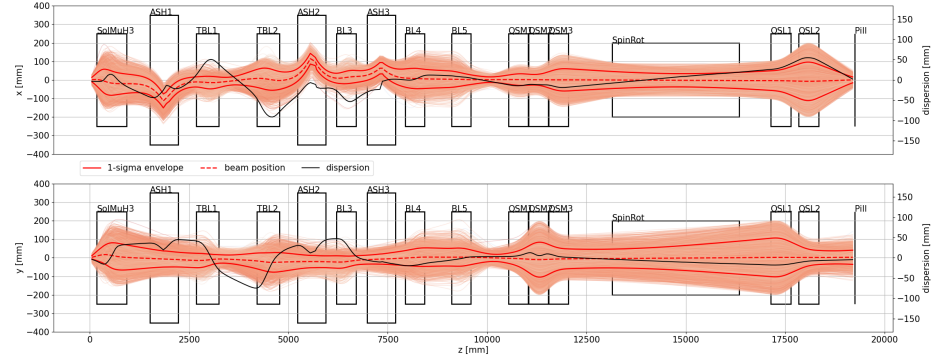

Rate @ 2.4 mA: 1.05e+09 μ^+/s
$x_{avg} = 0.24$ mm
STD(x_{avg}) = 15.83 mm
$xp_{avg} = 7.63$ mrad
STD(xp_{avg}) = 91.50 mrad
$y_{avg} = 2.84$ mm
STD(y_{avg}) = 38.28 mm
$yp_{avg} = 1.34$ mrad
STD(yp_{avg}) = 33.05 mrad
$\varepsilon_{x,\ 90\%} = 3.99\pi$ rad mm
$\varepsilon_{y,\ 90\%} = 4.54\pi$ rad mm
$P_{z,\ avg} = 27.50$ MeV/c
STD($P_{z,\ avg}$) = 1.36 MeV/c

Brightness: Muonium

Muonium yields for different emitters					
Beam	p [MeV/c]	1 σ [mm]	Aerogel back implantation	Aerogel, SiO_2 front implantation	SFHe source, front implantation
πE5	$\sim 10-20$	8.5	1.5×10^6	5.4×10^5	1.2×10^6
HIMB-cool	0.01	0.5	-	2×10^5	2.5×10^5

High quality intense muonium beams can be employed for high precision physics experiments:

- muonium spectroscopy
- antimatter gravity experiments

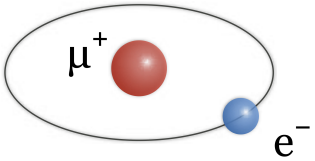

μSR: muon Spin Rotation

With μSR measurements it is possible to probe the magnetic properties of a material, and the energy of the muons define the depth in the sample.

HIMB would allow to:

- Increase the Low Energy muons (< 30 keV) rate by > 10: currently $\sim 4.5 \times 10^3$ μ/s, because they are degraded surface muons
- Allow to explore the sub-surface gap in depth: steep decrease in rate towards low momenta

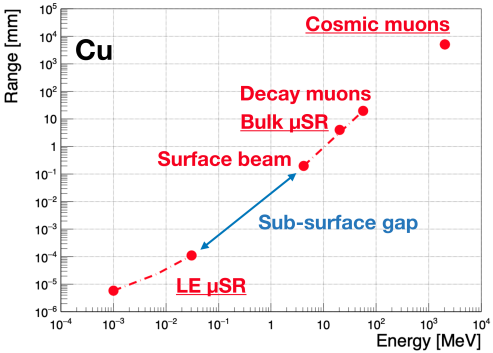

μSR: pixel detector

Together with higher muon rates, improvements on μSR technique are envised by introducing the use of silicon pixel sensors:

- low material budget
- muon vertexing (pile-up manageable)
- higher rates → lower measurement times and smaller/multiple samples

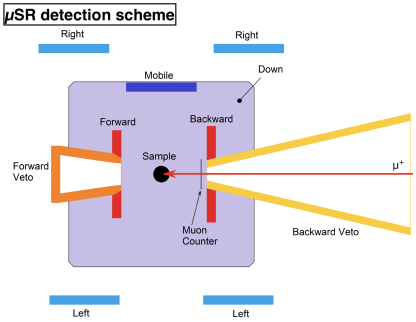

muCool

The muCool collaboration aims at developing a technique to compress surface μ^+ beams phase space by 10 orders of magnitude. This is possible by stopping the μ^+ in a helium atmosphere with a density gradient to then let them drift thanks to an $\vec{E} \times \vec{B}$ field.

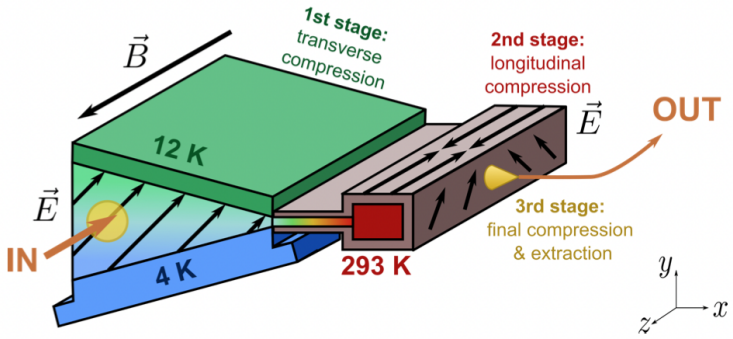

Lithium target

The target is a $2\,\mu m$ LiPON deposit on $25\,\mu m$ copper substrate.

A copper arm is used for both hold the target in position and to dissipate to the CW beamline the heat deposited by the proton beam.

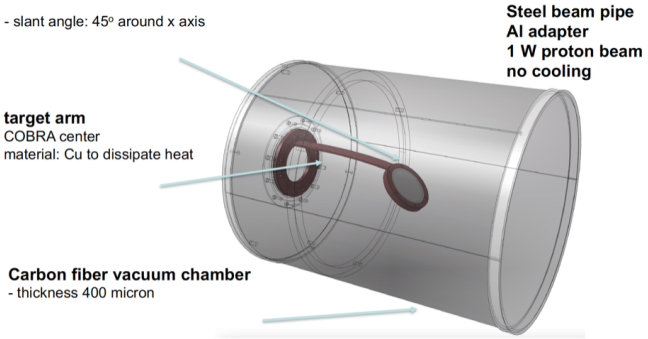

Likelihood definition

$$\log \mathcal{L} = \log \mathcal{L}_{data} + \log \mathcal{L}_{nuisance} \quad (2)$$

$$= \sum_{i=1}^{n} D_i \log f_i - f_i + \sum_{i=1}^{n} \sum_{j=1}^{m} a_{ji} \log A_{ji} - A_{ji} + \sum^{k} \frac{\alpha_k^2}{2\sigma_k^2} \quad (3)$$

- D_i is the population in the data i-th data bin
- f_i is the estimated population in the i-th bin
- a_{ji} is the observed statistics in the j-th MC sample in bin i
- A_{ji} is the estimator of a_{ji}

Beeston-Barlow

The estimated population is linked to the nuisance parameter by the population strengths:

$$f_i = \sum_{j=1}^{m} p_j A_{ji} \tag{4}$$

$$p_j = \frac{\hat{\mathcal{N}}_{j,data}}{\mathcal{N}_{j,MC}} \tag{5}$$

To minimize the likelihood with this many nuisances, it is possible to separately do the minimization:

- MIGRAD minimizes the yields
- for each set of evaluated yields, the likelihood is minimized against the A_{ji}s

To find the best A_{ji}s for a given set of yields there is an analytical expression and for each bin a mono-dimensional non-linear equation can be solved. The ideal is to use the BRENTQ method:

$$\frac{D_i}{1-t_i} = \sum_{j=1}^{m} \frac{p_j a_{ji}}{1+p_j t_i}, \quad \text{solve for } t_i \tag{6}$$

Null-bins treatment

The nuisances are then given by:

$$A_{ji} = \frac{p_j a_{ji}}{1 + p_j t_i} \tag{7}$$

Such machinery is needed when the MC population is lower in size then 10 times the data size, which means for $p_j > 0.1$. In such cases it is frequent to have empty bins in MC production, so $a_{ji} = 0$. The correct treatment is to modify only the highest strength null bin:

$$t_i = -\frac{1}{p_k} \tag{8}$$

$$A_{ki} = \frac{D_i}{1 + p_k} - \sum_{j \neq k} \frac{p_j a_{ji}}{p_k - p_j} \tag{9}$$

If $A_{ki} <= 0$ no action is taken and the normal procedure is used. This is analogous to the case when the difference between the data and some of the other populations is statistically negligible.

Sensitivity estimate

The UL on the X17 yield in case of the null hypothesis is here computed on 100 Toy Experiments. **The two template scenario give the same sensitivity.**

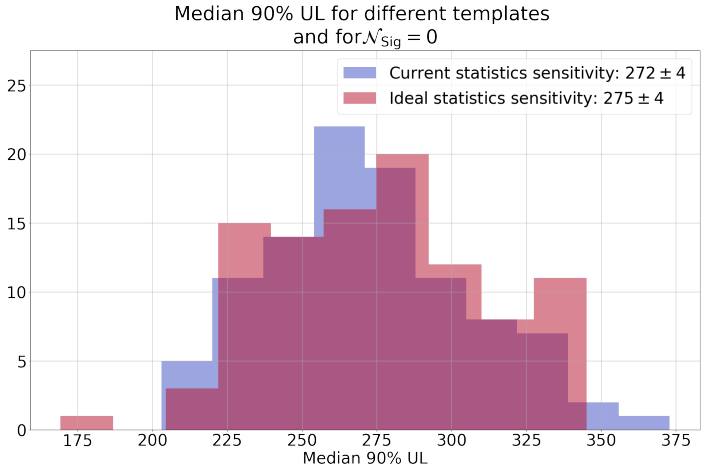

Sensitivity estimate - sanity check

The same was done for $\hat{\mathcal{N}}_{\mathrm{Sig}} = 450$. **The ideal statistic scenario gives better limits than the current one as expected.**

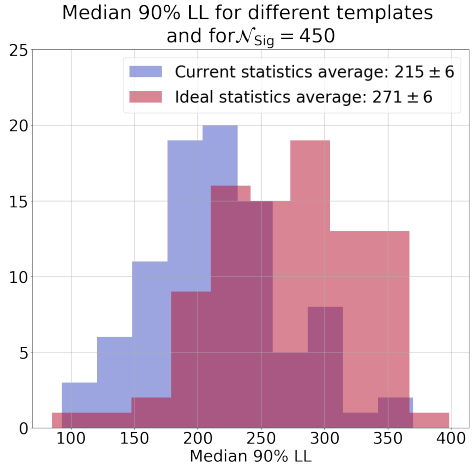

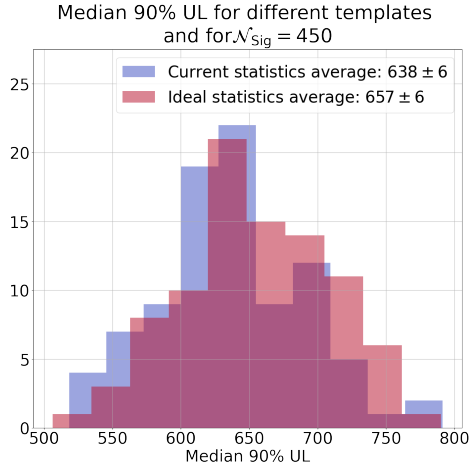

Beeston-Barlow lite

The Beeston-Barlow approach accounts for uncertainty statistics by fitting each bin of each population with a Poisson PDF.

This is good to correctly account for the combination of their uncertainty, but similar performances can be achieved by including the statistical uncertainty of the total estimate only.

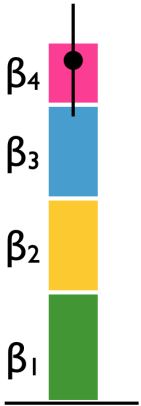

(a) BB Complete

(b) BB Lite

Beeston-Barlow lite

In this approach, a multiplicative factor is introduced to model the statistical fluctuations due to systematics. Two possible approaches are:

- Conway's: the factor is Gauss distributed. The bin likelihood is:

$$\log \mathcal{L}_i = D_i \log \beta_i f_i - \beta_i f_i - \frac{(\beta_i - 1)^2}{2\sigma^2_{\beta_i}} \quad (10)$$

$$\sigma_{\beta_i} = \frac{\sigma_{f_i}}{f_i} \quad (11)$$

- Dembinski-Abdelmotteleb's: the factor is Poisson distributed. The bin likelihood is:

$$\log \mathcal{L}_i = D_i \log \beta_i f_i - \beta_i f_i + f_{i,eff} \log \beta_i f_{i,eff} - \beta_i f_{i,eff} \quad (12)$$

$$f_{i,eff} = \left(\frac{f_i}{\sigma_{f_i}} \right)^2 \rightarrow \beta_i = \frac{D_i + f_{i,eff}}{f_i + f_{i,eff}} \quad (13)$$

with $f_{i,eff}$ the number of Poisson distributed events which have a relative uncertainty equal to f_i.

Beryllium lines

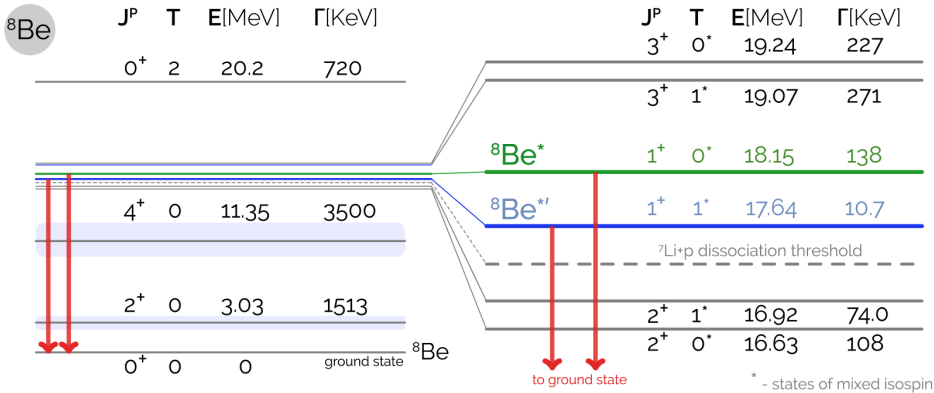

Gauge coupling limits

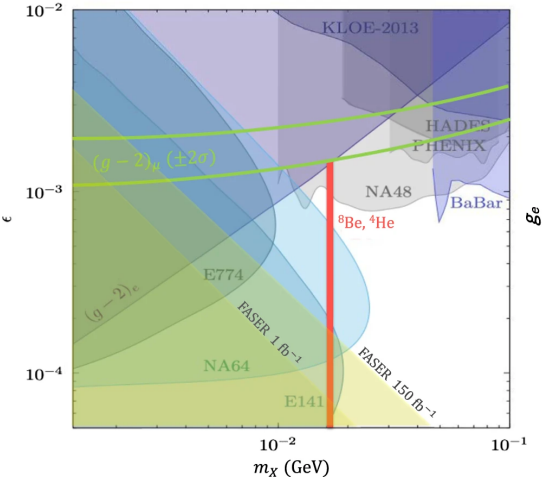

(a) all limits

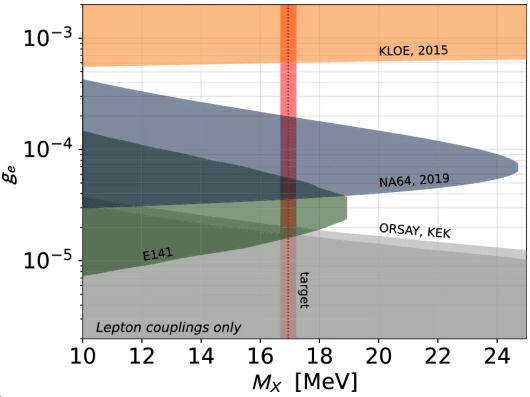

(b) lepton couplings only